NASA TECHNICAL MEMORANDUM NASA TM-77755

NON-DESTRUCTIVE EVALUATION TECHNIQUES HIGH TEMPERATURE CERAMIC COMPONENT PARTS FOR GAS TURBINES

H. Reiter, S. Hirsekorn, J. Lottermoser, K. Goebbels

Translation of "ZfP von Hochtemperatur-Keramik-Bauteilen für KfZ-Turbinen", Fraunhofer-Institut für Zerstörungsfreie Prüfverfahren, Saarbruecken, West Germany, Report IzfP-800305-TW, March 6, 1980

NATIONAL AERONAUTICS AND SPACE ADMINISTRATION
WASHINGTON, D.C. 20546 September 1984

STANDARD TITLE PAGE

1. Report No. NASA TM-77755	2. Government Accession No.	3. Recipient's Catalog No.
4. Title and Subtitle NON-DESTRUCTIVE EVALUATION TECHNIQUES - HIGH TEMPERATURE CERAMIC COMPONENT PARTS FOR GAS TURBINES		5. Report Date September 1984
		6. Performing Organization Code
7. Author(s) H. Reiter, S. Hirsekorn, J. Lottermoser, K. Goebbels Fraunhofer Institute for NDE		8. Performing Organization Report No.
		10. Work Unit No.
9. Performing Organization Name and Address Leo Kanner Associates, Redwood City, California 94063		11. Contract or Grant No. NASW-3199
		13. Type of Report and Period Covered Translation
12. Sponsoring Agency Name and Address National Aeronautics and Space Administration, Washington, D.C. 20546		14. Sponsoring Agency Code

15. Supplementary Notes

Translation of "ZfP von Hochtemperature-Keramik-Bauteilen für KfZ-Turbinen", Fraunhofer-Institut für Zerstörungsfreie Prüfverfahren, Saarbruecken, West Germany, Report IzfP-800305-TW, March 6, 1980

16. Abstract

This report concerns studies conducted on various tests undertaken on material without destroying the material, including microradiographic techniques, vibration analysis, high-frequency ultrasonic tests with the addition of evaluation of defects and structure through analysis of ultrasonic scattering data, microwave tests and analysis of sound emission.

17. Key Words (Selected by Author(s))		18. Distribution Statement Unclassified-Unlimited	
19. Security Classif. (of this report) Unclassified	20. Security Classif. (of this page) Unclassified	21. No. of Pages	22. Price

NASA-HQ

NON-DESTRUCTIVE EVALUATION TECHNIQUES HIGH TEMPERATURE CERAMIC COMPONENT PARTS FOR GAS TURBINES

H. Reiter, S. Hirsekorn, J. Lottermoser, K. Goebbels
Fraunhofer Institute for NDE

Contents

The present report deals with the studies conducted in 1979 within the second phase on the techniques appearing to be most promising in the first phase: /1*

- Microradiographics
- Vibration analysis
- High frequency ultrasound

as well as several studies not conducted up to that time:

- Defect and structure assessment through analysis of ultrasonic scattering data
- Microwave tests
- Analysis of sound emission.

The resolution capacity was optimized through microradiographic techniques. This includes, on the one hand, mechanical means for adjusting the sample (sample table with horizontal and vertical movement capabilities, rotation of the sample) and film cassette mounts or image amplification adjustment (setting of the geometric distance relationships, direct enlargement). On the other hand, the correct adjustment of energy and exposure parameters (mA x time) in relation to film and foil combinations as well as type, geometry and wall thickness of the irradiated object also belong to optimization.

An improvement in the test arrangement for the vibration analysis - design and construction of an appropriate support and an impact transmitter - led to results which could be reproduced even for complex geometries (turbine blades).

*Numbers in the margin indicate pagination in the foreign text.

In addition to the RH heads with piezoelectrically vaporized layers [2] a further possibility was tested of generating ultrasonic waves of high frequency through the electrical excitation of $LiTaO_3$ single crystals. Tests with the ultrasonic microscope SLAM demonstrated the suitability for describing structural inhomogeneities and defect detection in Si_3N_4 and SiC with ultrasonic waves of 100 MHz.

The studies on ultrasonic propagation in multiple-phase systems is a possibility for recognizing defects and assessing structure. Reflection, scattering, bending and absorption supply statements on the scattering object and the structure of the observed medium.

The studies with microwaves and the sound emission test did not supply any satisfactory results on defect detection and characterisation of the material with the presently employed experimental set-up and evaluation techniques.

Both measurement set-ups (RF and SLAM) are necessary for the evaluation of structure and the detection of defects and the set-ups supplement one another. The RF measurement set-up is suitable for detecting very minute individual defects and offers the possibility of signal processing on the receiver side. Digitalisation and subsequent inverse filtration first via software and later via hardware in a black box will improve the resolution capacity. The commercially available SLAM, however, provides more rapid scanning of components with large surface areas and therefore permits a fast description of the structure and a corresponding quicker location of defects. It analyzes macroscopic volumes with microscopic resolution, somewhat comparable to microradiographic techniques. /23

In addition to this activity in the area of ultrasonics, there is a plan to supplement the series of studies conducted with one further method before concluding the project. Application of the heat conduction procedure for non-destructive techniques of high temperature ceramics SiC and Si_3N_4 will be tested.

8. Tables and Figures

Concept for a classification of defects in high temperature ceramics in relation to components and load:
(See following page for key)

1 Belastung 2 Bauteil	Temperature 15 (z.B. Thermoschock)	25 Zug, Druck, Scher (z.B. Flieh-, Einsp.-Kräfte)	29 Korrosion (z.B. Heißgasangriff)
3 Brennkammer, 4 Flammrohr 5 Wandstärke- änderungen 6 Bohrungen	16 Risse	26 Einspannung	30 amorphe SiO_2- Schichten innere Oxidation
7 Einlaufkonus, -spirale 5 Wandstärke- änderungen 8 Kanten	17 Geometrieunter- schiede 16 Risse 18 Klebestelle 7 (Einlaufspirale)	26 Einspannung	30 amorphe SiO_2- Schichten innere Oxidation
9 Leitkranz 10 innerer, äußerer Ring 11 Schaufeln	17 Geometrieunter- unterschiede 19 ungleichmäßige thermische Aus- dehnung leading-, trailing edge		30 amorphe SiO_2- Schichten innere Oxidation 31 Oberflächenfehler
Rotor 12 HP-Nabe+-Schaufeln 13 HP-RB-Verbund 14 RB-Schaufeln	20 Thermoschockrisse 21 Kriechen, langsames 22 Geometrieänderungen 23 Bindefehler 24 unterschiedliche Wärmeausdehnung leading-, trailing edge	27 Exzentrizität, Reibung Rißwachstum 23 Bindefehler 26 Einspannung 28 Schaufelkante, -fuß	31 Oberflächenfehler 30 amorphe SiO_2- Schichten innere Oxidation

Key:
1. load
2. component
3. combustion chamber
4. flue
5. alteration in wall thickness
6. holes
7. inlet cone, spiral
8. edges
9. guide rim
10. inner and outer ring
11. blades
12. HP hub + blades
13. HP-RB combination
14. RB blades
15. e.g. thermal shock
16. cracks
17. geometrical differences
18. adhesion point
19. uneven thermal expansion
20. thermal shock cracks
21. crawling, slow formation of cracks
22. alterations in geometry
23. defects in binding
24. differing heat expansion
25. push, pull, cutting (e.g. centrifugal, clamping forces)
26. clamping
27. eccentricity, friction
28. blade edge, base
29. corrosion (e.g. attack by hot gas)
30. amorphous SiO_2 layers, internal oxidation
31. surface defects

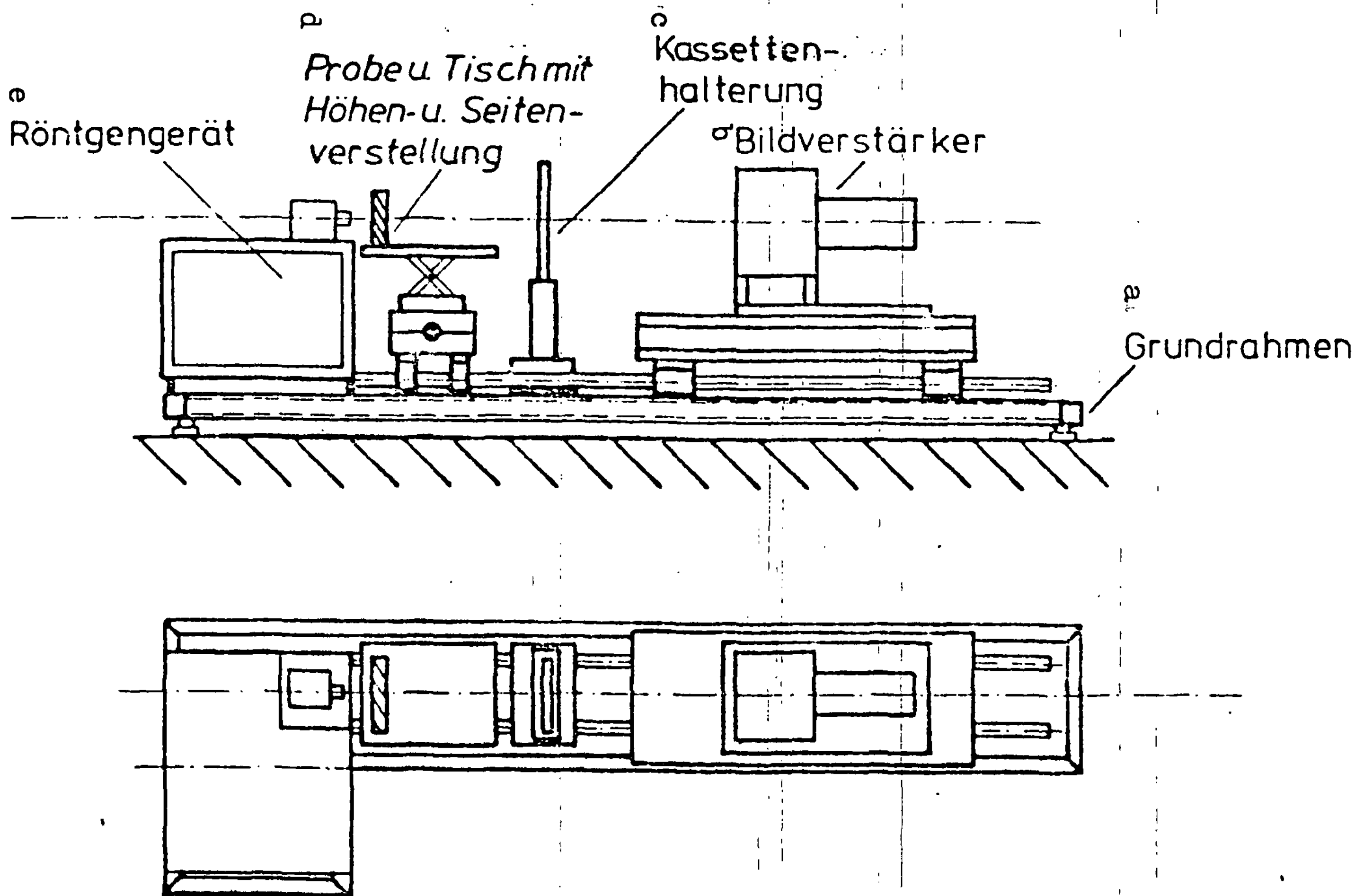

Fig. 1: Sketch of the Microradiographic Set-Up

Key:
- a. basic frame
- b. image amplifier
- c. casette mounting
- d. Sample and table with adjustment in heigth and in lateral direction
- e. X-ray instrument

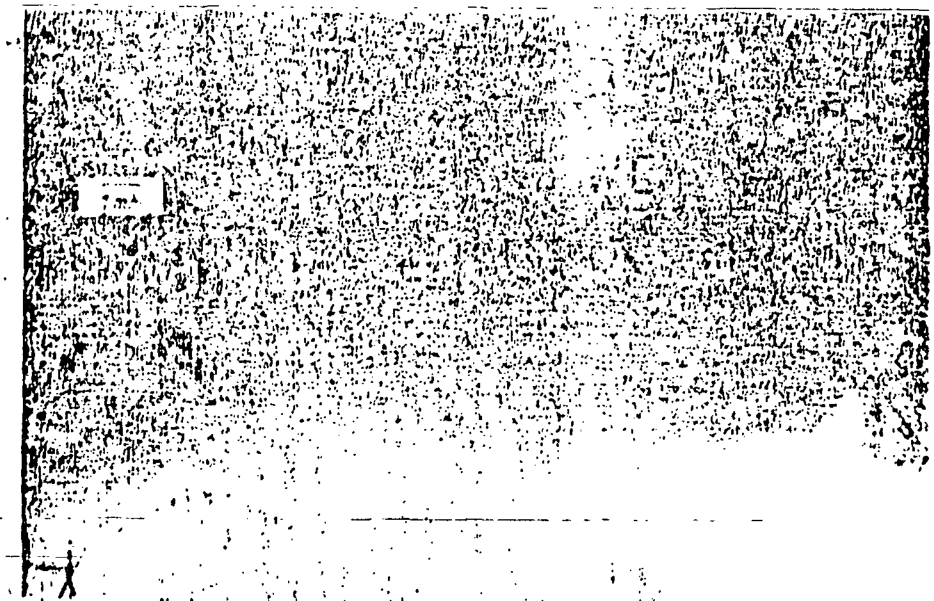

Abb. 2a

a HPSC-Scheibe, 5,7mm Dicke, WC-Einschluß

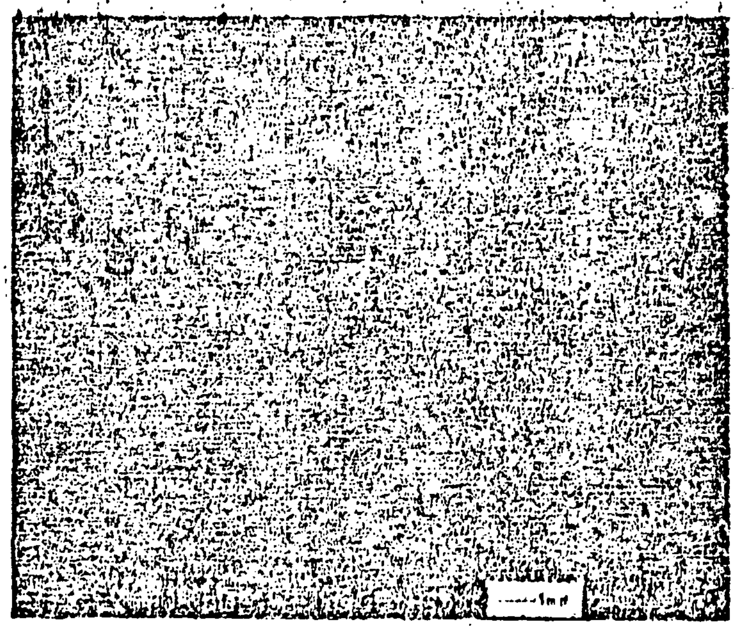

Fe

Abb. 2b

b 2 HPSN-Proben, Fe-und C-Einschluß

c 1 HPSC-Probe, Fe-Einschluß (von links nach rechts)

Fig. 2: Microradiogram of HPSC and HPSN Samples with artificially applied Defect Points

Key: a. HPSC disc, 5.7 mm thickness, WC Inclusion
b. 2 HPSN Samples, Fe and C Inclusion
c. 1 HPSC Sample, Fe Inclusion (from the left to the right)

Abb. 3a

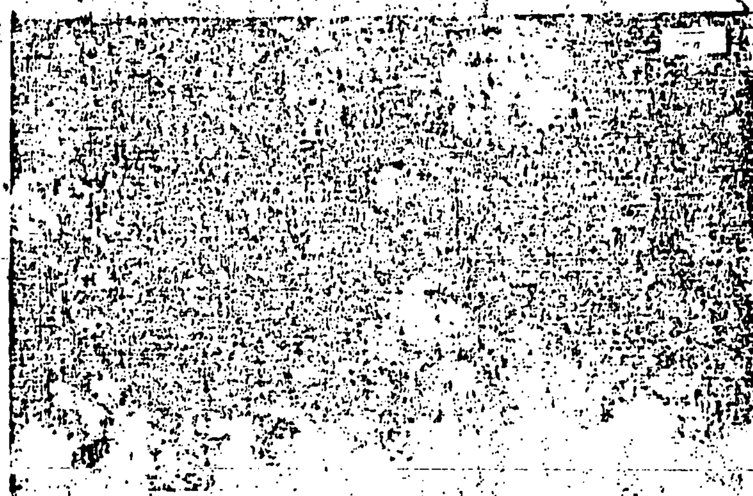

Abb. 3b

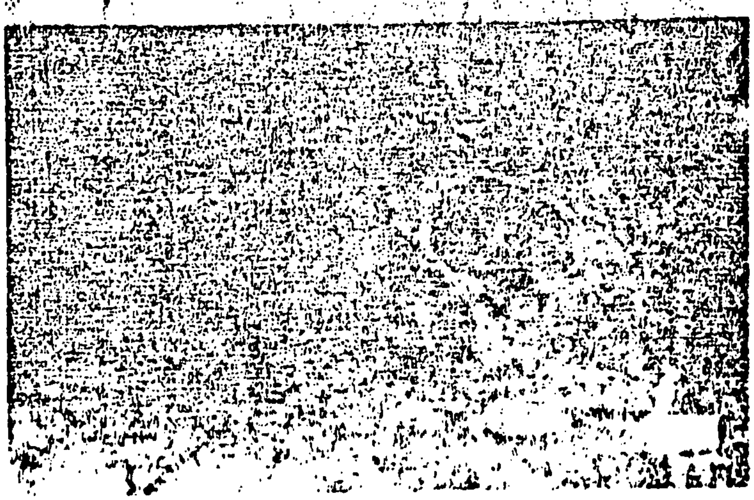

Abb. 3c

Fig. 3: SiC Pipes with different Content of Silicon, increasing from a to c.

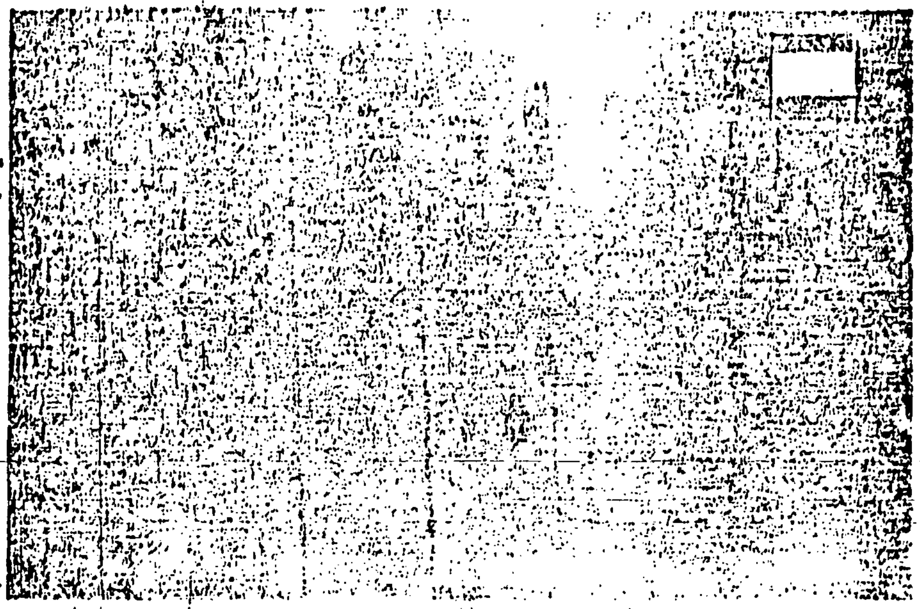

. Abb. 4a

a ohne Optimierung

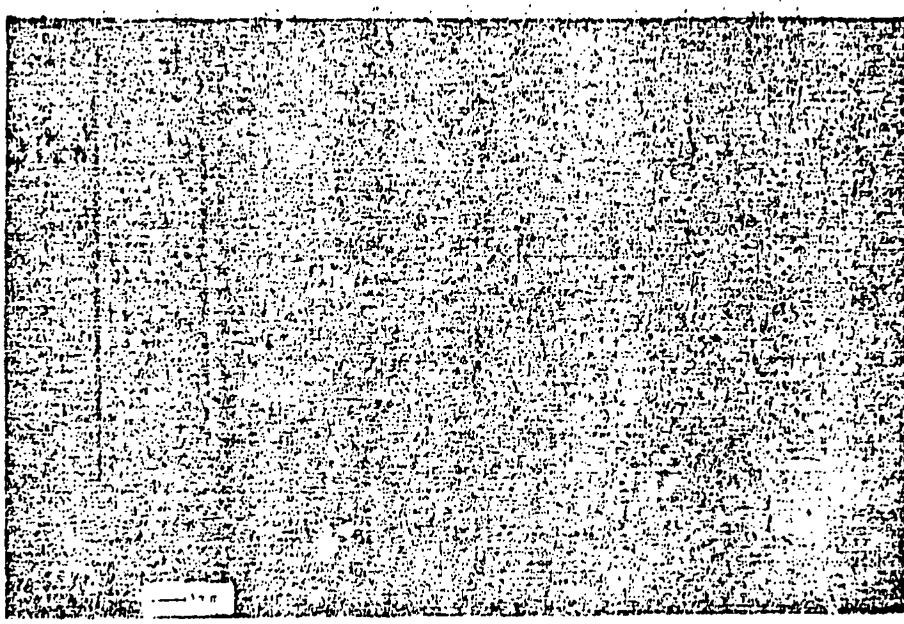

Abb. 4b

b nach erfolgter Optimierung

Fig. 4: RBSN Centrifugal Disc with Saw Cuttings

Key: a. without optimizing
b. after optimizing

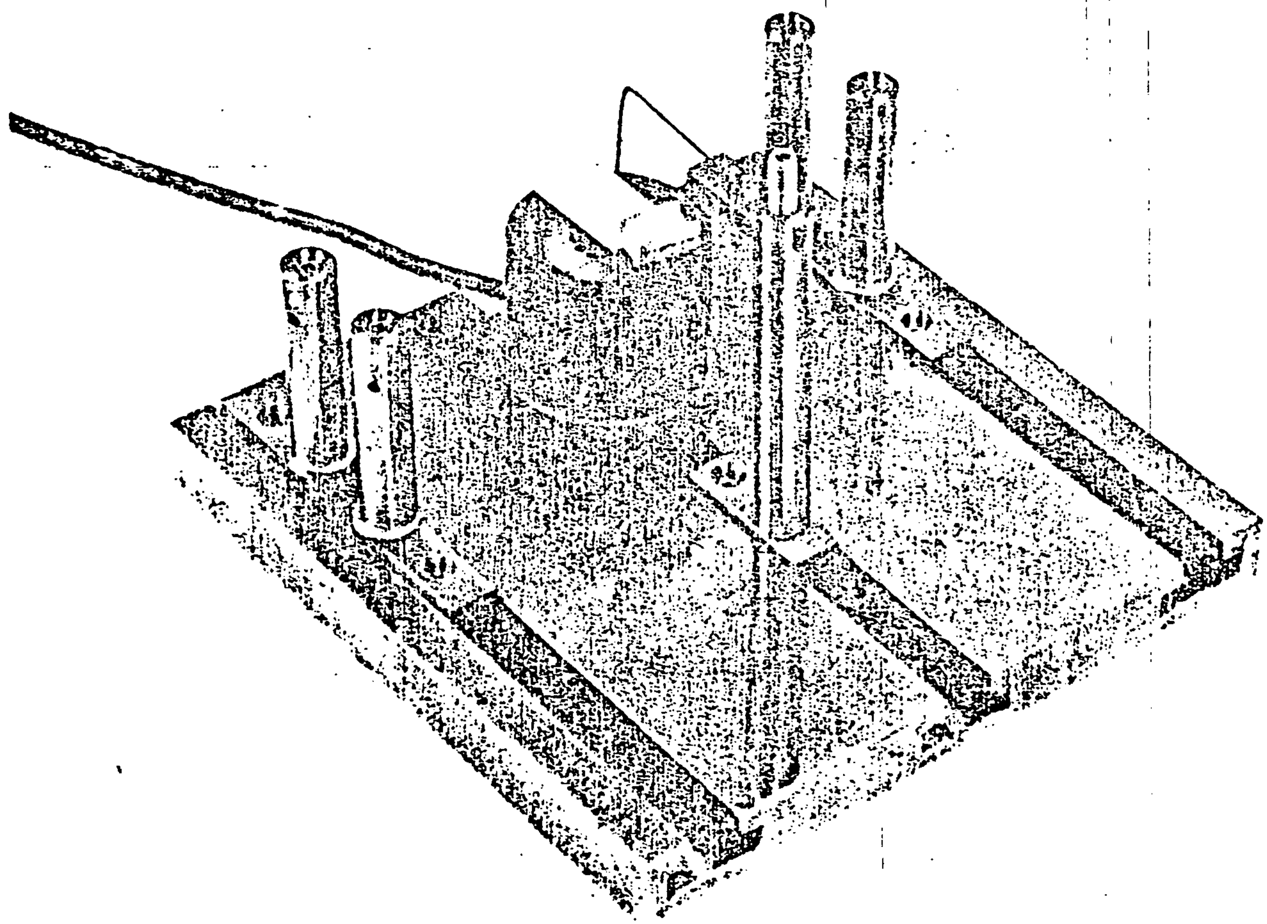

IzfP

Fig. 5: Support and Impact Transmitter in the Vibration Analysis

Abb. 5

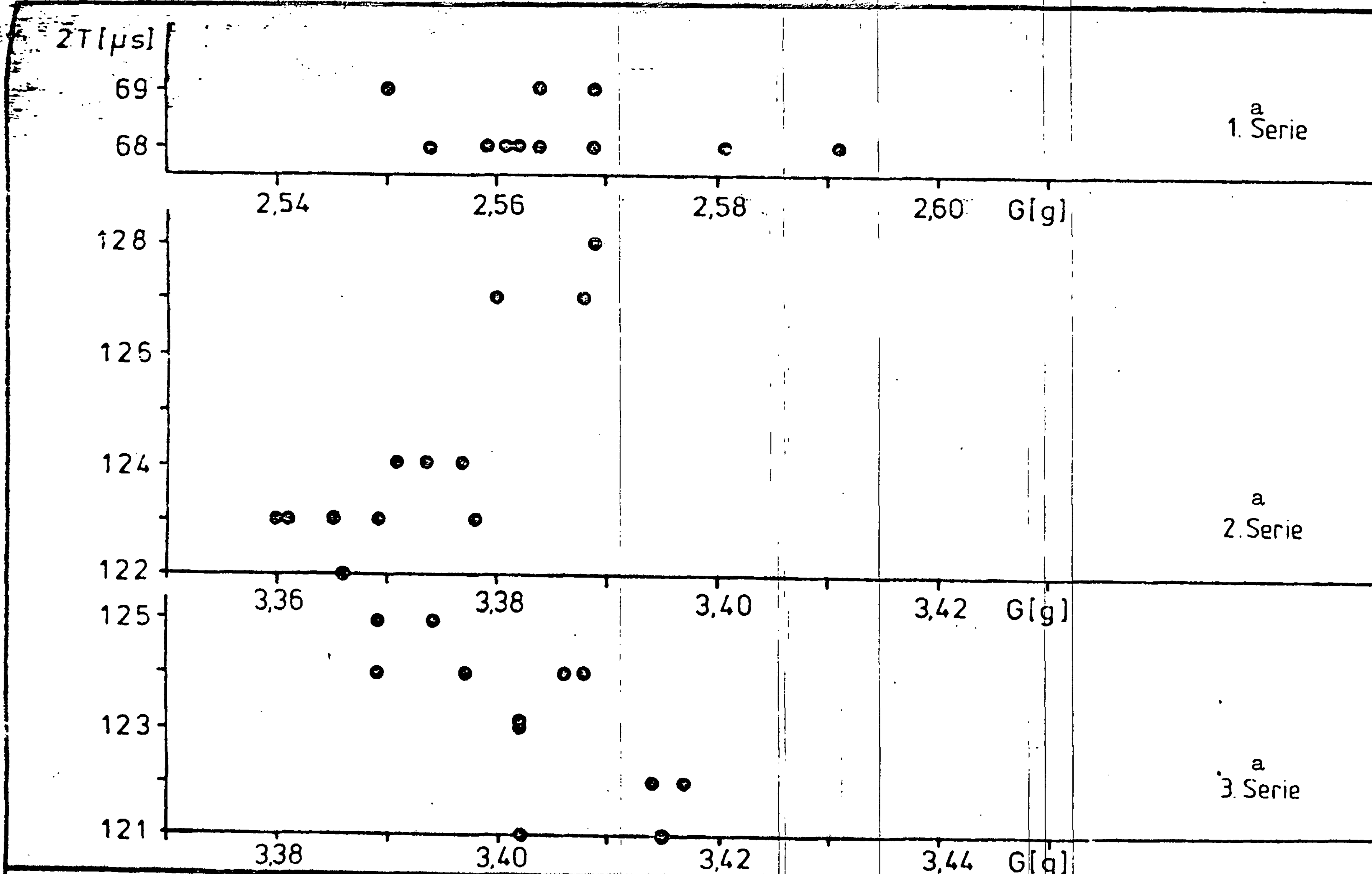

IzfP

Fig. 6: Vibration Analysis with RBSN Blades
Key: a. series

Abb. 6

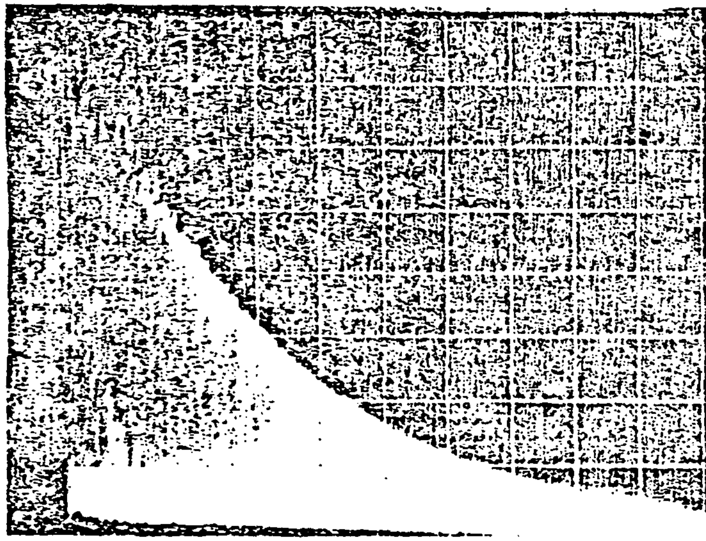

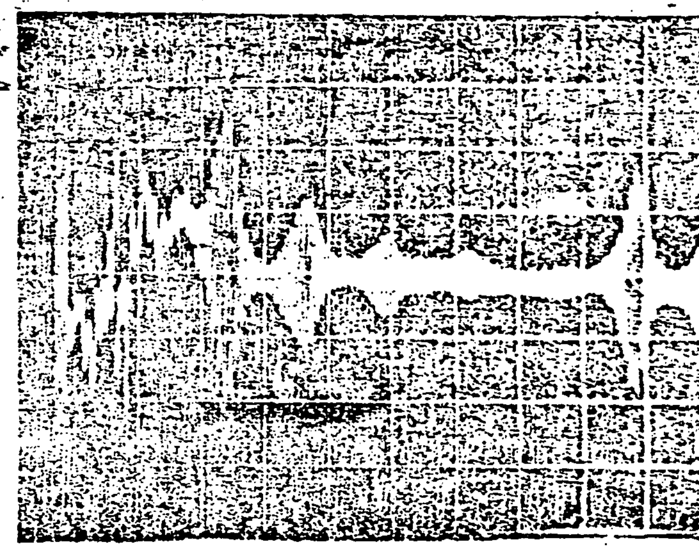

[a]Rückwandechos, $LiTaO_3$
90 MHz

Key: a. rear wall echo
b. and
c. sample
d. thickness

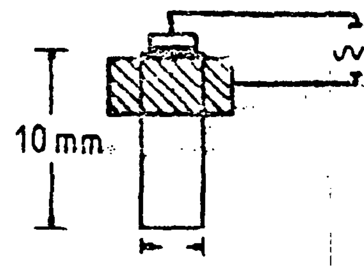

[a] Rückwandechos, $LiTaO_3$ [b] und
HPSN [c] Probe, [d] Dicke: 3,5 mm
20 MHz

IzfP

Fig. 7: High Frequency Ultrasound with a $LiTaO_3$ Converter

Abb. 7

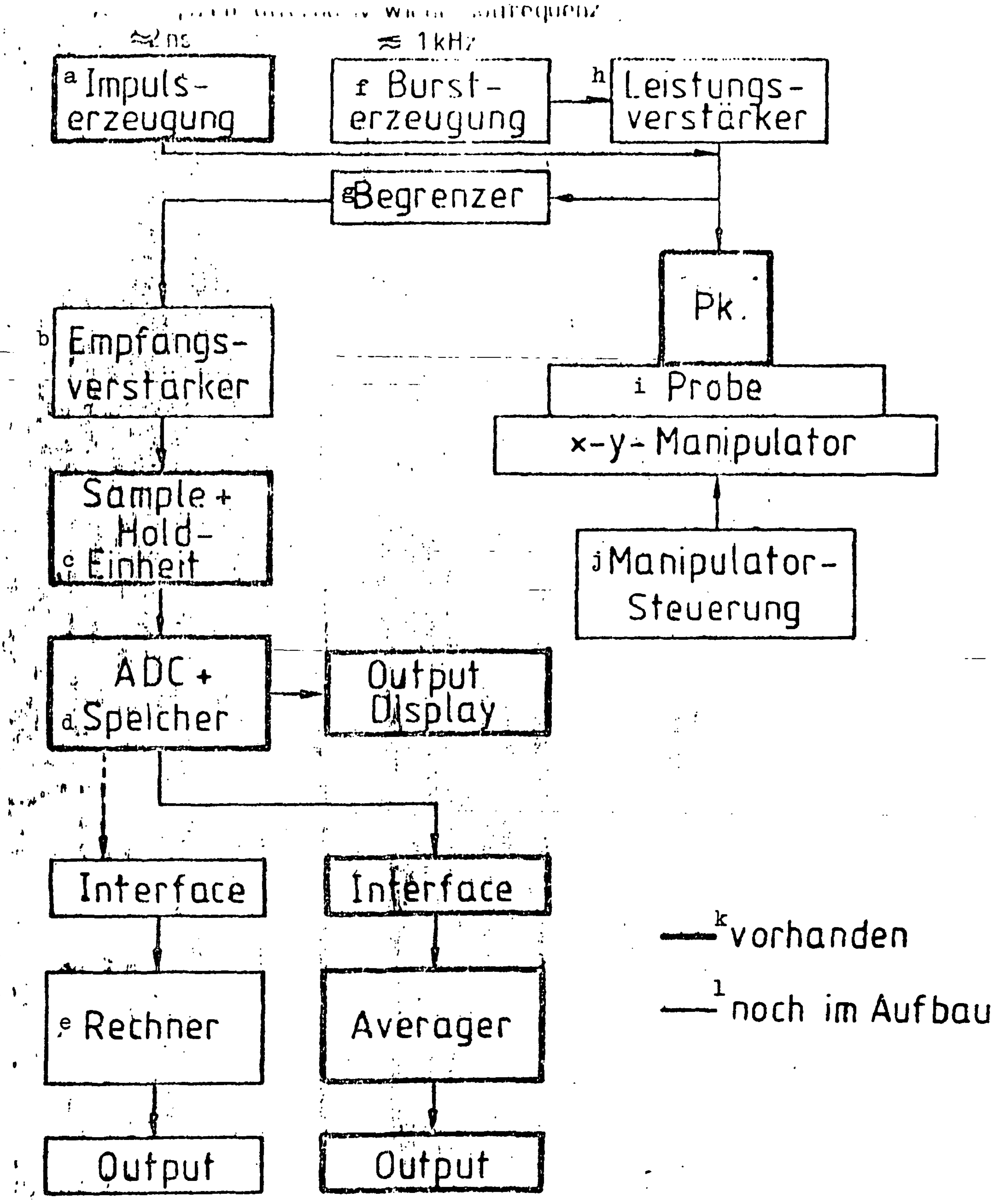

Fig. 8: Block Diagram of High Frequency Ultrasonic Measurement Set-Up (≤ 150 MHz)

See following page for key.

Key for Fig. 8:

a. generation of impulse
b. receiver amplification
c. unit
d. store
e. computer
f. generation of burst
g. limiter
h. output amplification
i. sample
j. manipulator control
k. already present
l. under construction

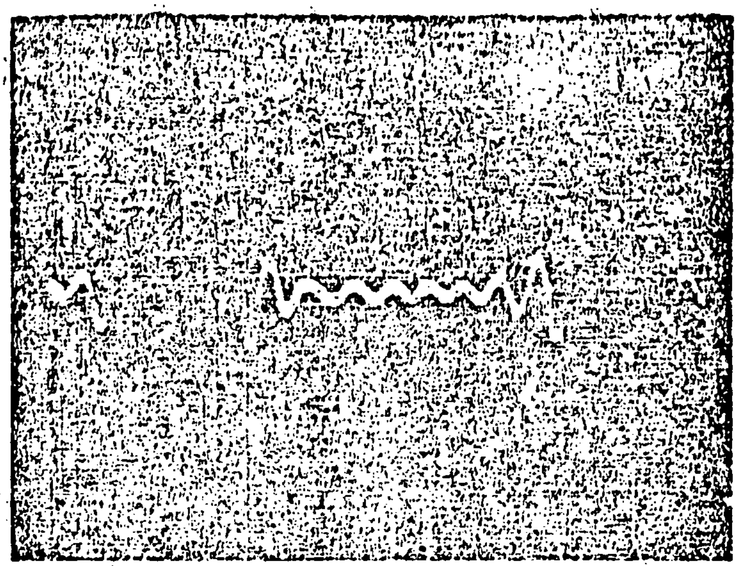

Abb. 9 a

a HPSC-Probe, fehlerfreie Stelle

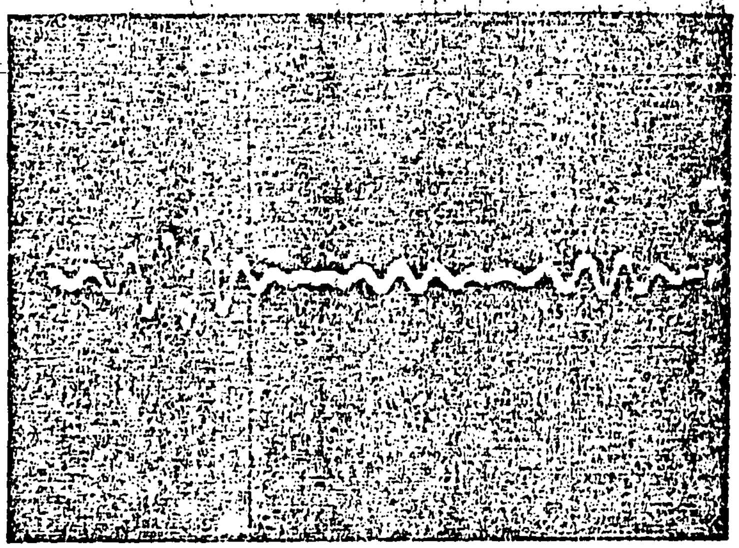

Abb. 9 b

b HPSC - Probe, Fe - Einschluß

Fig. 9: Ultrasonic Test of a 3.5 mm thick HPSC rod with Fe Inclusion, 16 MHz

Key: a. HPSC sample, free of defects
b. HPSC sample, Fe inclusion

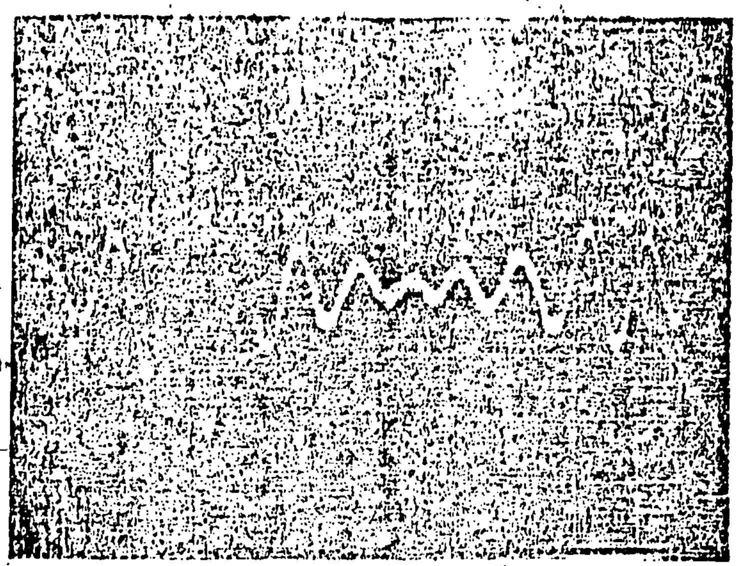

0,1 µs
20 mV

Abb.10 a

a HPSN-Probe, fehlerfreie Stelle

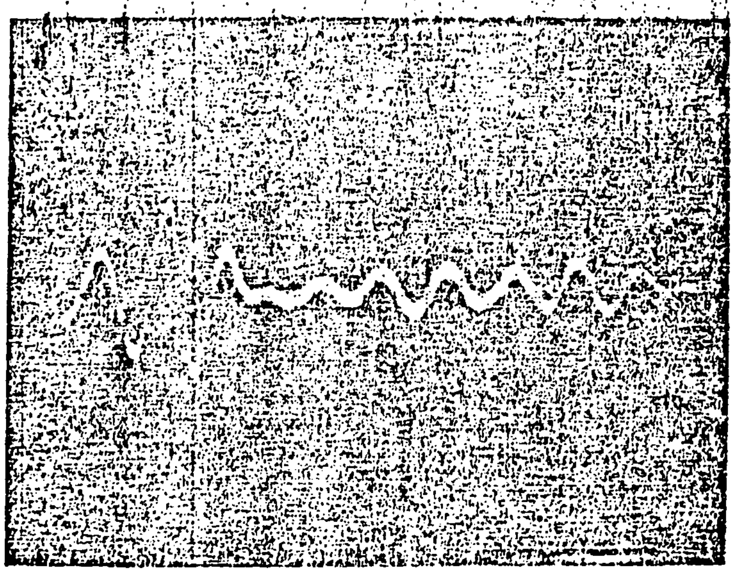

0,1 µs
20 mV

Abb.10 b

b HPSN-Probe, C-Einschluß

Fig. 10: Ultrasonic Test of a 3.5 thick HPSN rod
with C inclusion, 16 MHz

Key: a. HPSN sample free of defects
b. HPSN sample, C inclusion

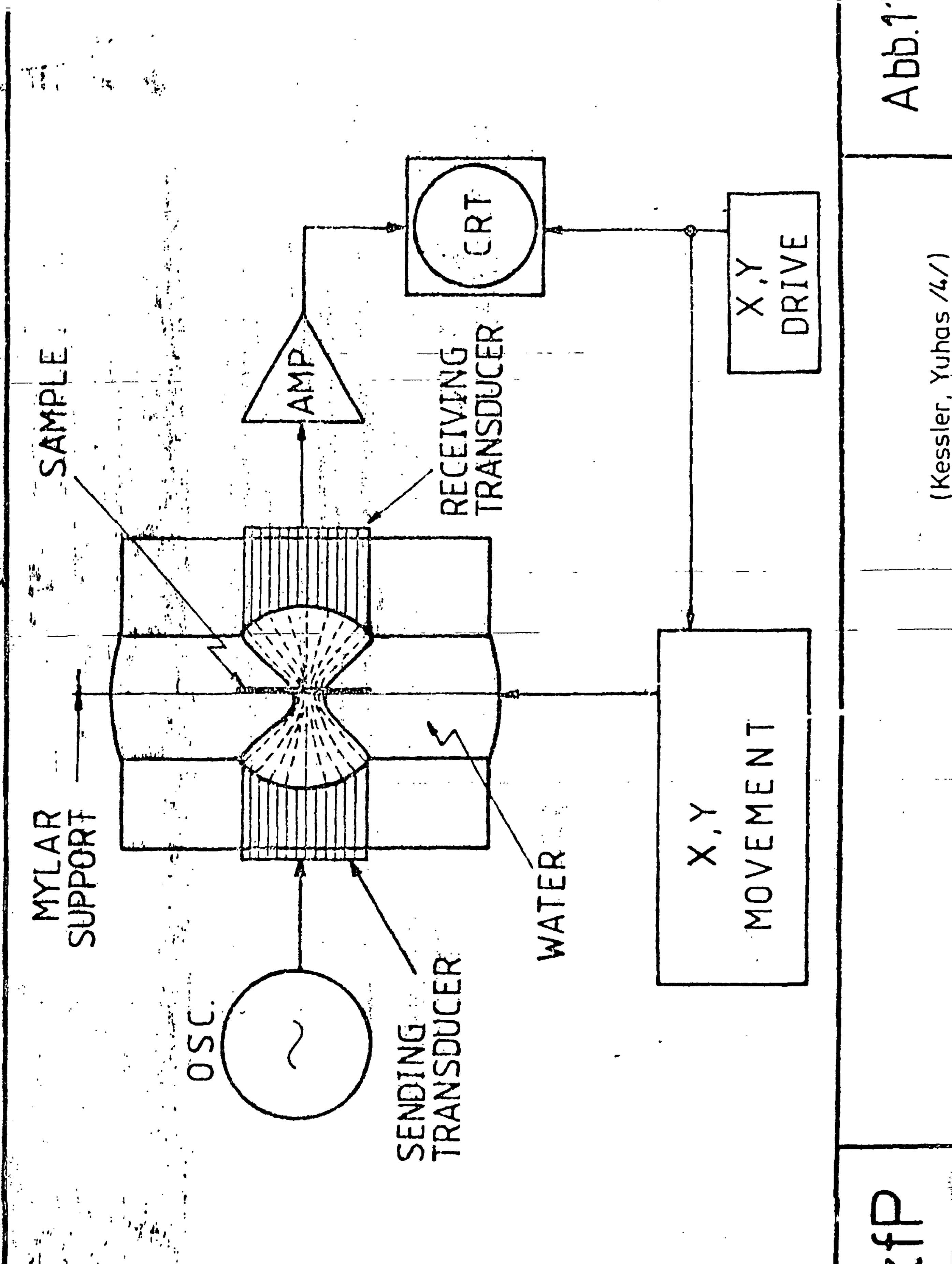

Fig. 11: Mode of Function of SAM

IzfP

Schematisches Diagramm SLAM

(Kessler, Yuhas /4/)

Abb.

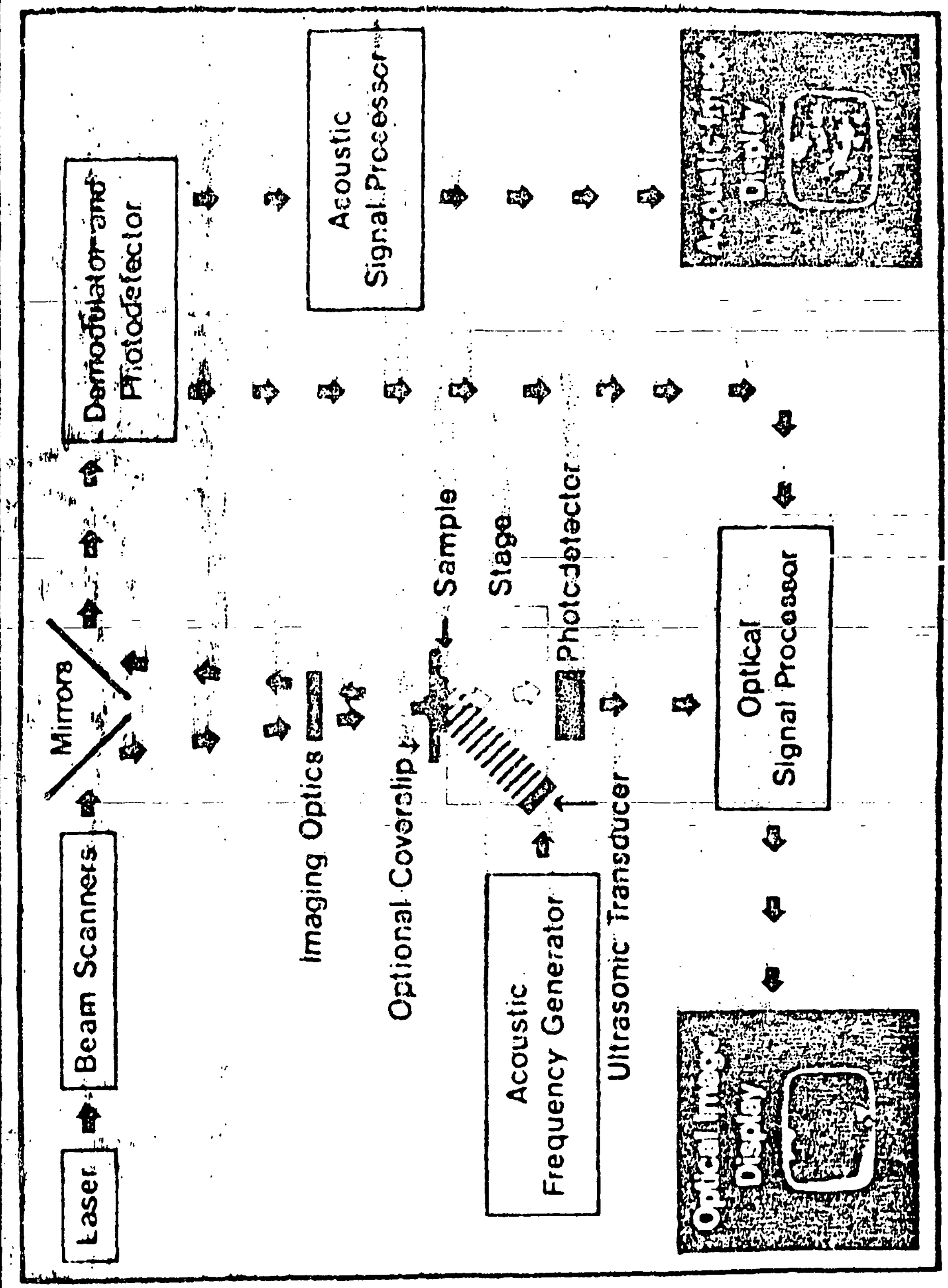

Fig. 12: Schematic Diagram of the SLAM

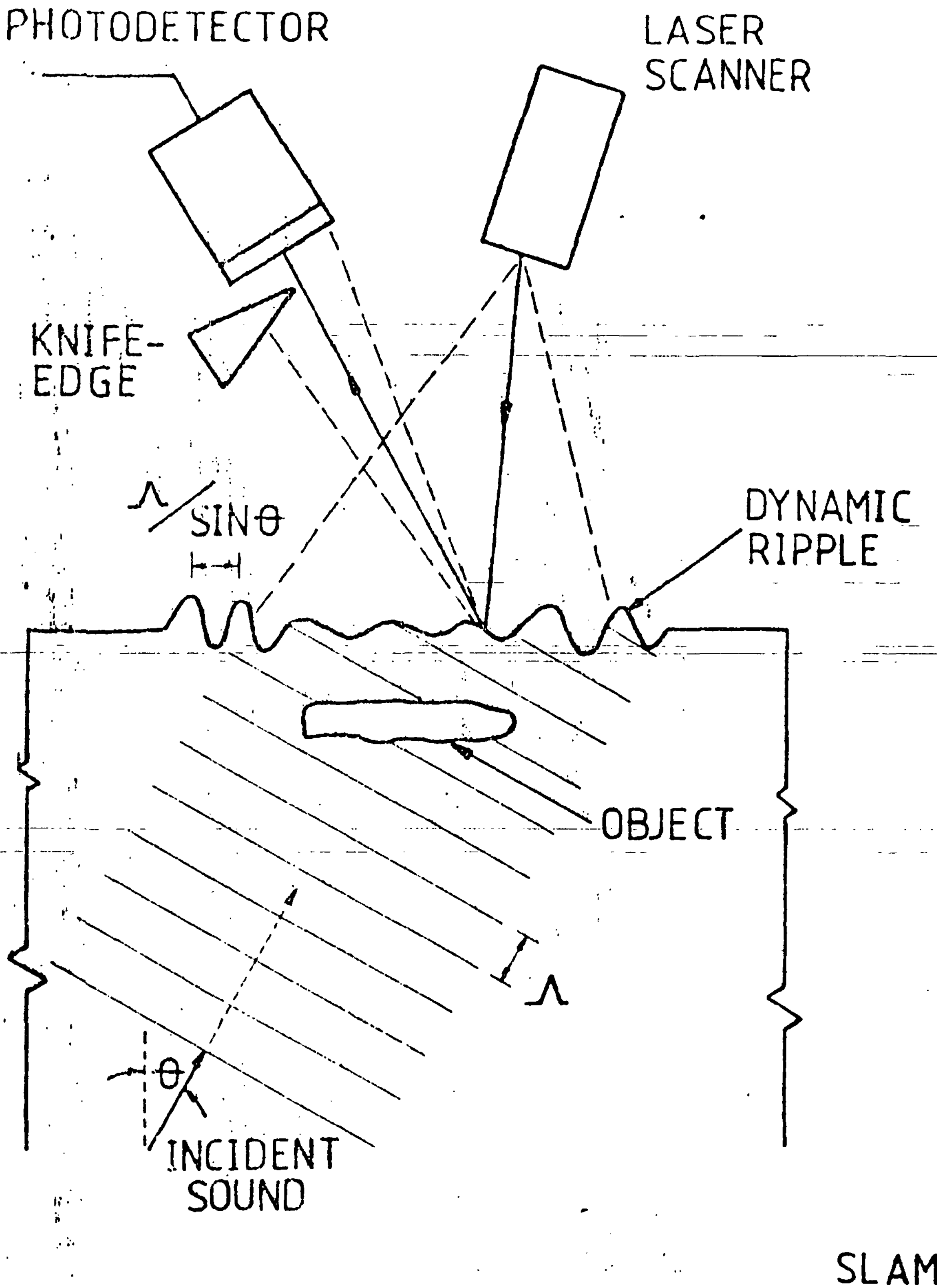

Fig. 13: Detection of acoustic energy at the boundary surface by means of the laser.

a Einschluß

Abb. 14 a

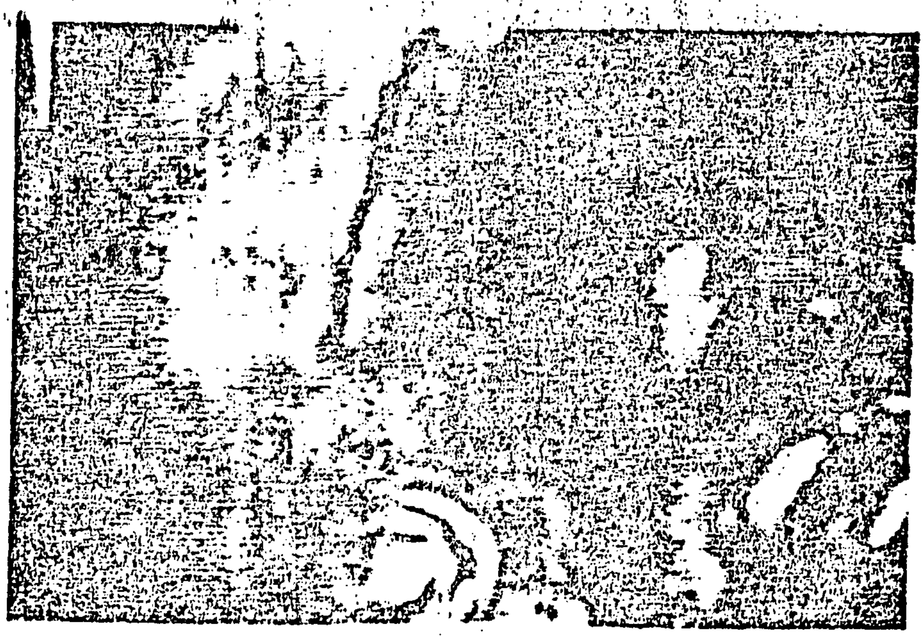

b Oberflächenschäden

Abb. 14 b

Fig. 14: SLAM Photos of defect points in a HPSC disc.

Key: a. Inclusion
b. Surface damage

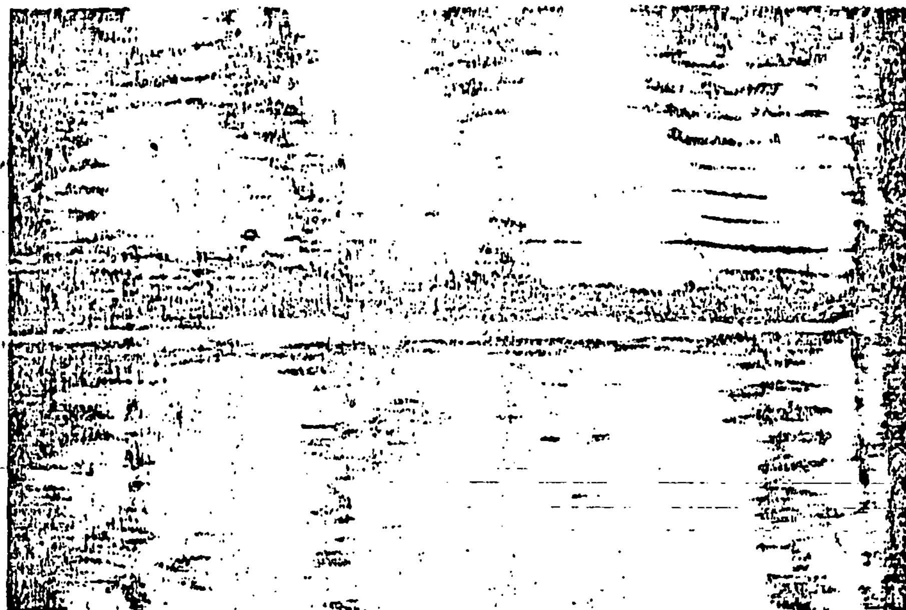

Abb. 15a

a Sägeschnitt 150·50 µm²

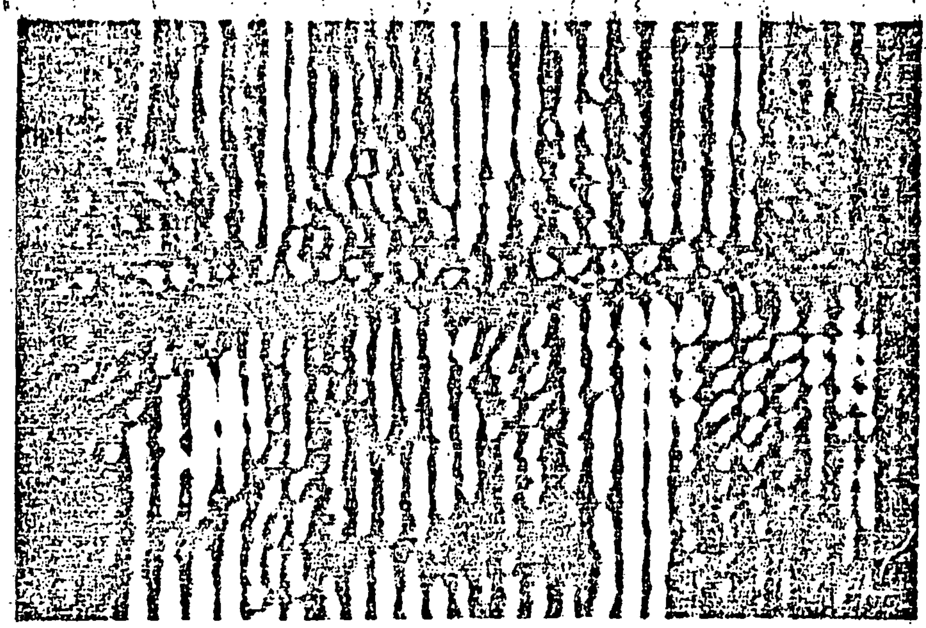

Abb. 15b

b. interferometrische Darstellung

Fig. 15: SLAM Photo of a saw cutting in a HPSN sample.

Key: a. saw cutting
b. interferometic representation

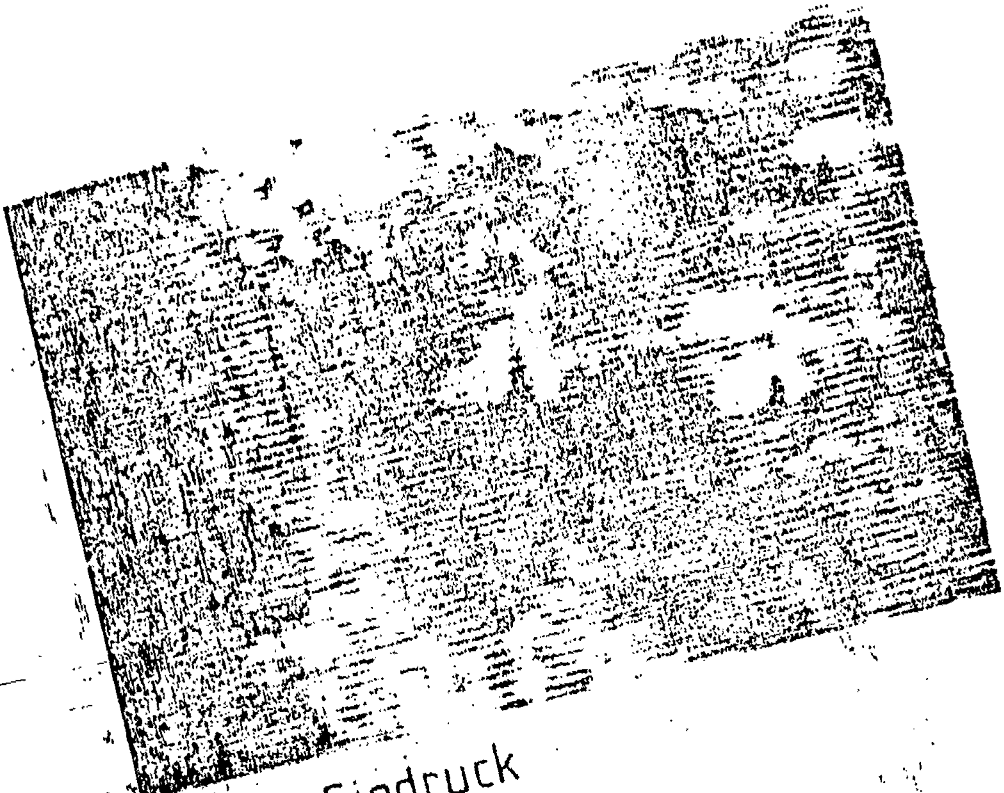

Abb. 16a

a Knoop - Eindruck

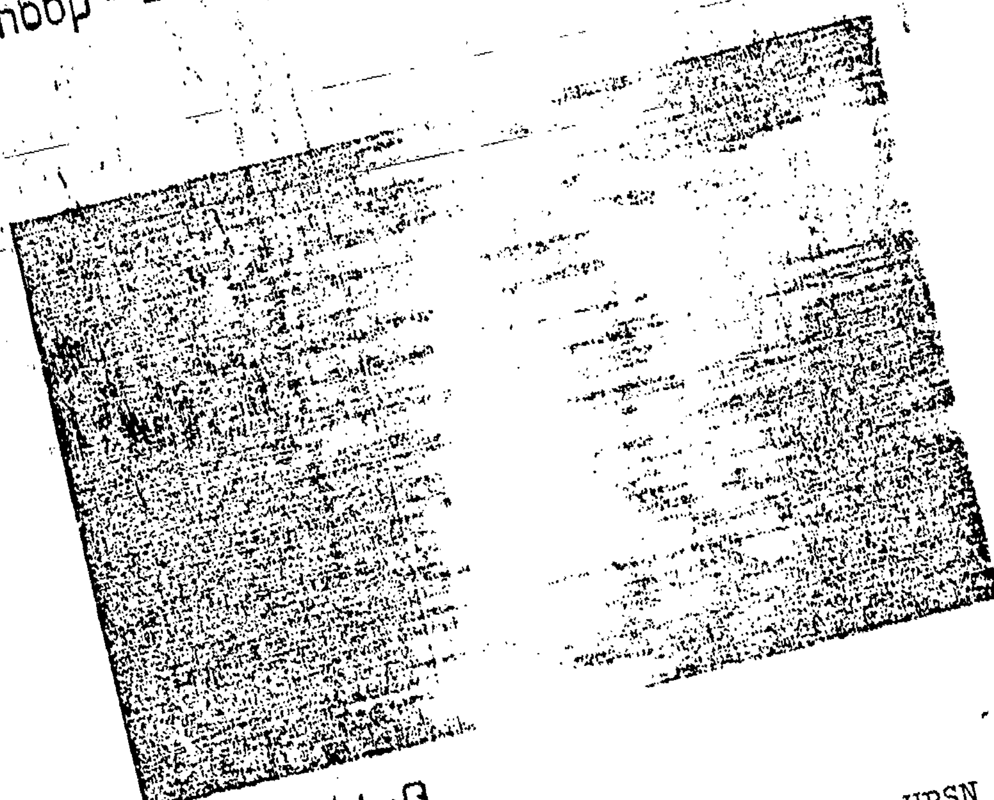

Abb. 16b

b C-Einschluß

Fig. 16: SLAM Photos of defects in HPSN samples.

Key: a. Knoop impression
b. C inclusion

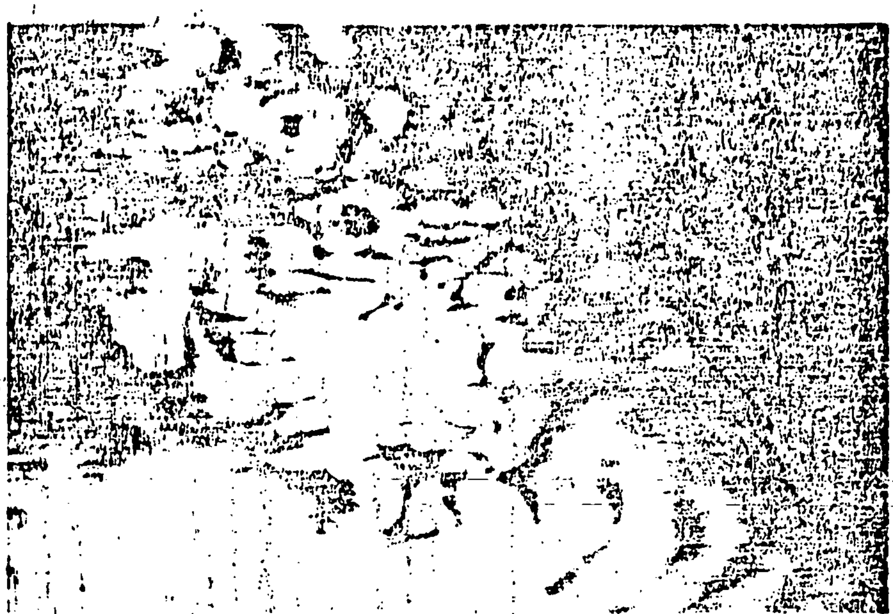

Abb. 17a

a HPSC-Probe mit Fe-Einschluß

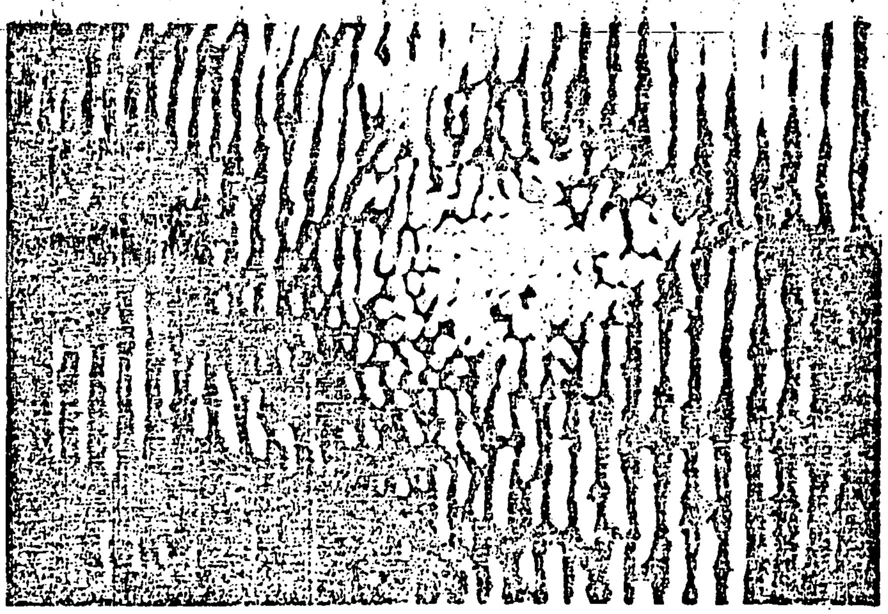

Abb. 17b

b HPSC-Probe mit Fe-Einschluß, interferometrische Darstellung

Fig. 17: SLAM Photo of an Fe inclusion in an HPSC sample.

Key: a. HPSC sample with Fe inclusion
b. HPSC sample with Fe inclusion, interferometric representation

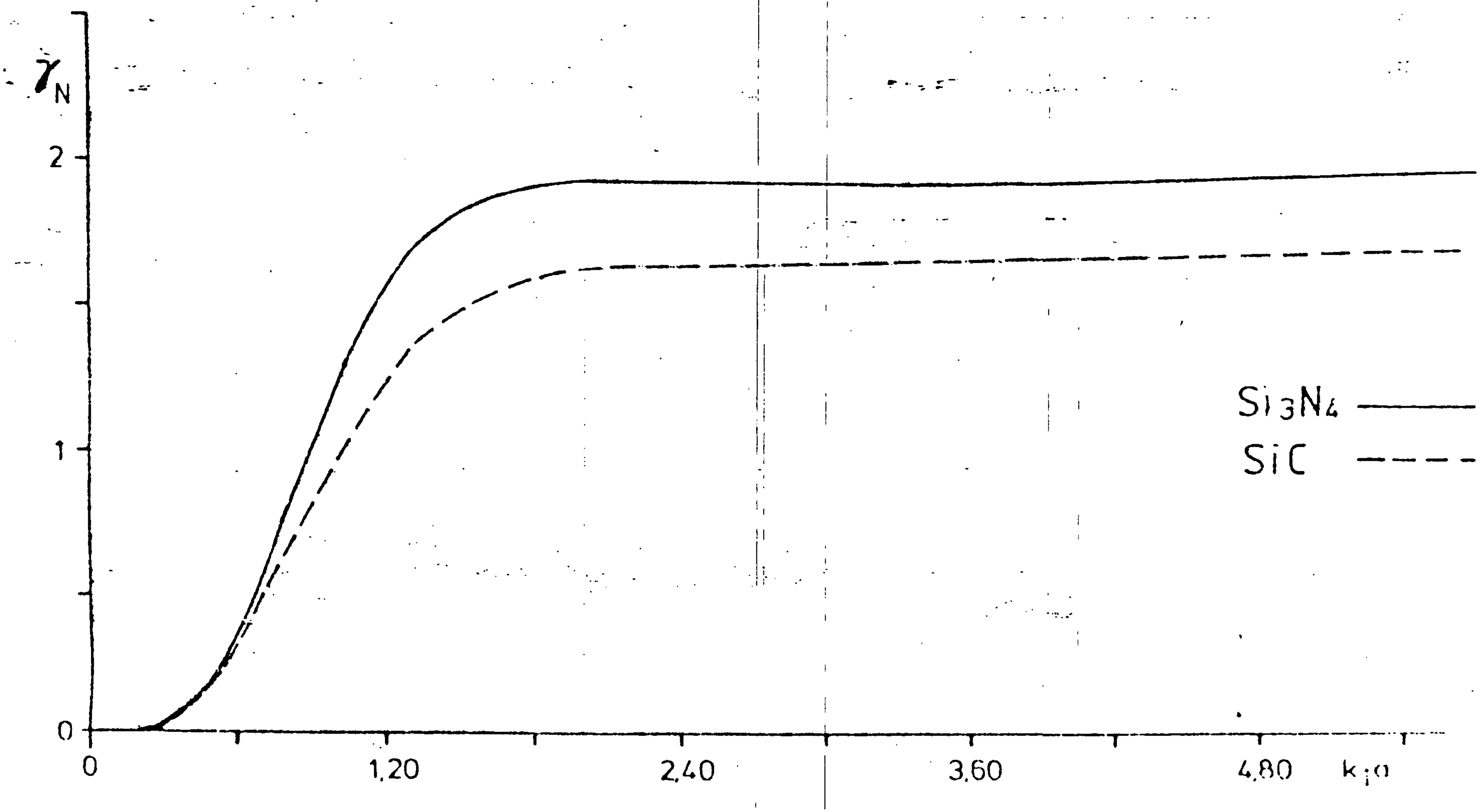

IzfP

Fig. 18: Standardized scattering cross-section γ_N for pores in the case of incident longitudinal wave

Abb. 1

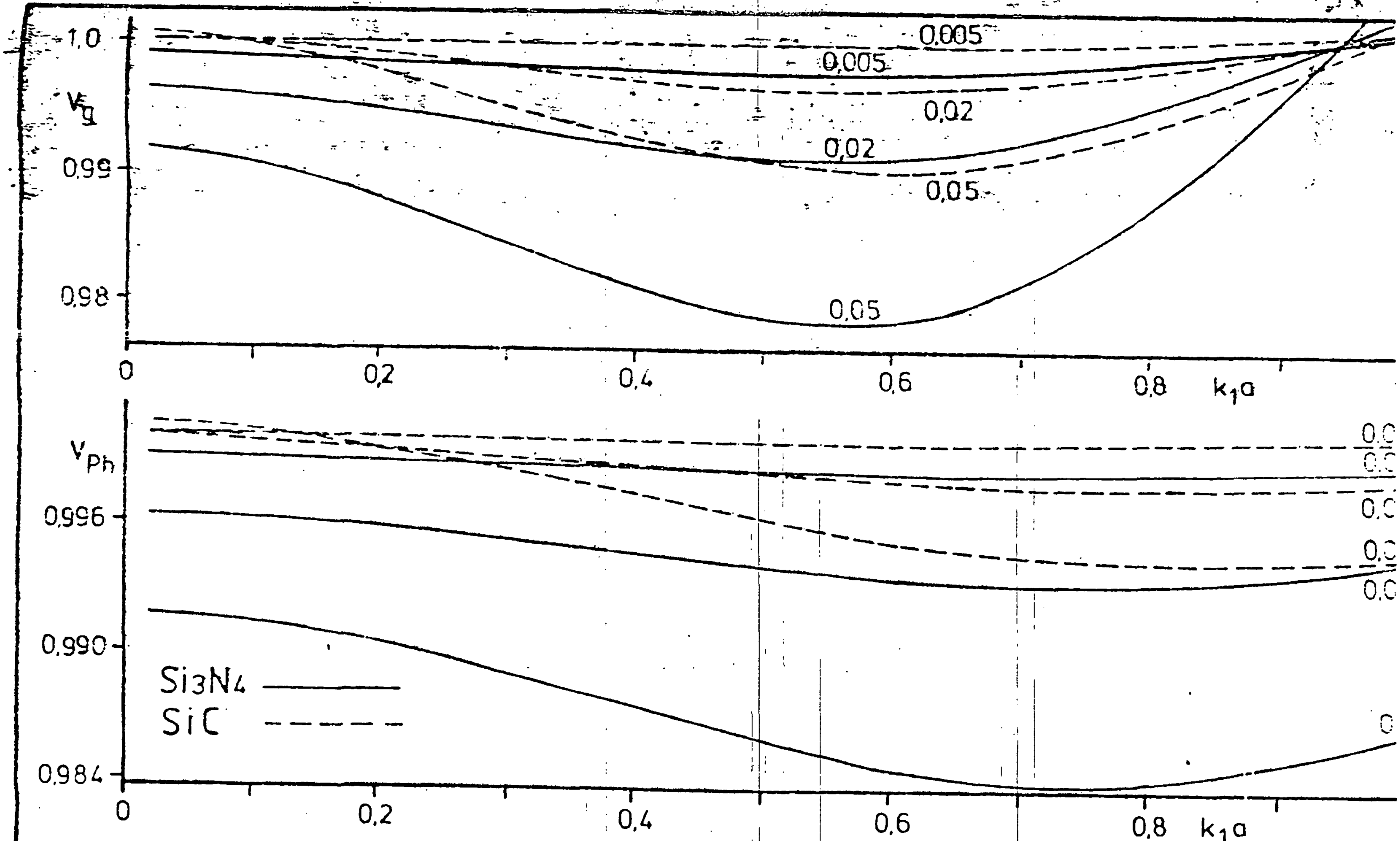

IzfP

Fig. 20: Standardized longitudinal group and phase velocity v_g and v_{Ph} for various volume parts of scattering.

Abb.20

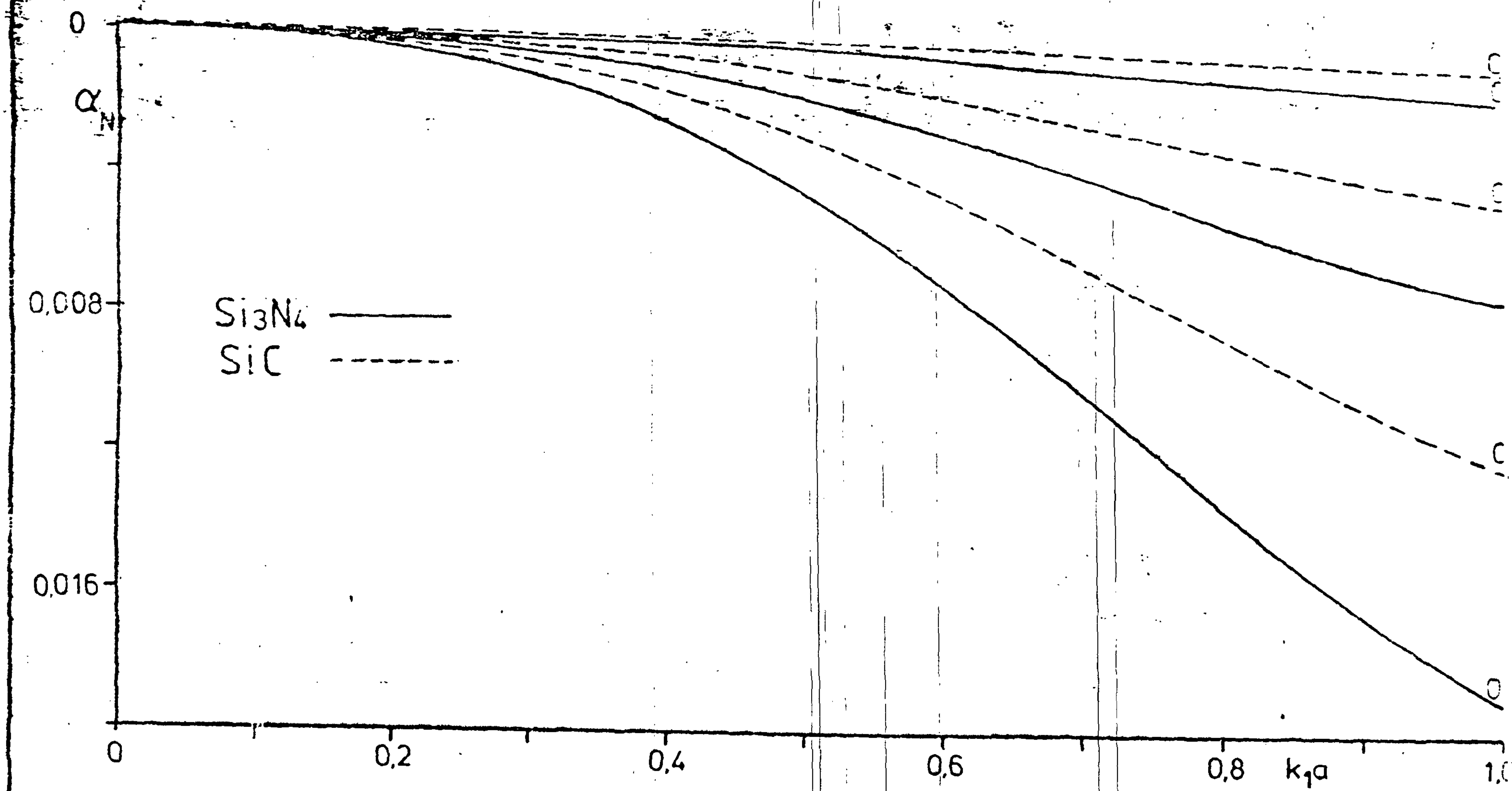

IzfP

Fig. 21: Standardized dispersion coefficient α_N in the case of incident longitudinal wave.

Abb. 21

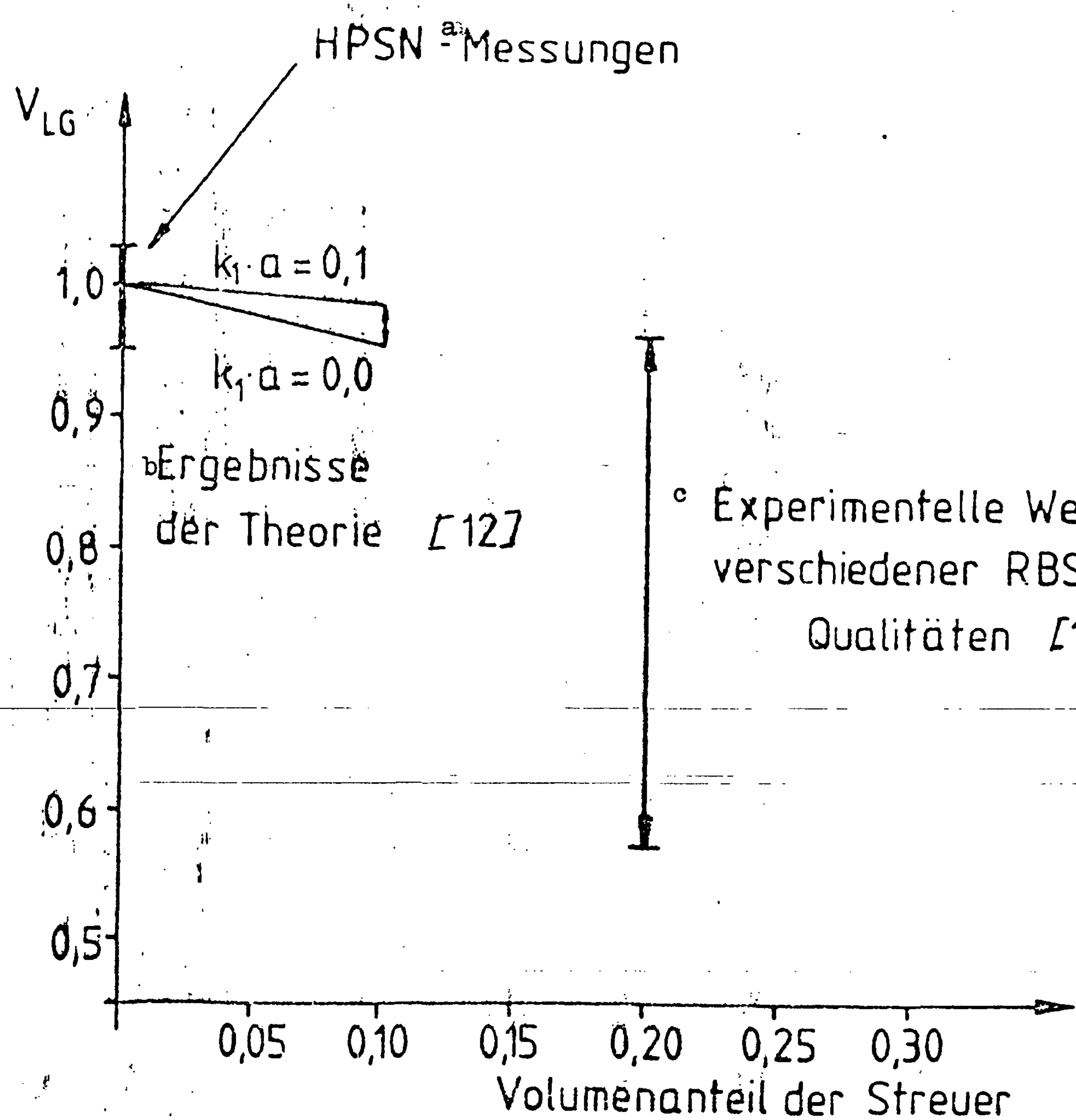

Fig. 22: Standardized longitudinal group velocity, theoretical and experimental values; Si_3N_4

Key: a. measurements
b. theoretical results
c. experimental values of various RBSN qualities

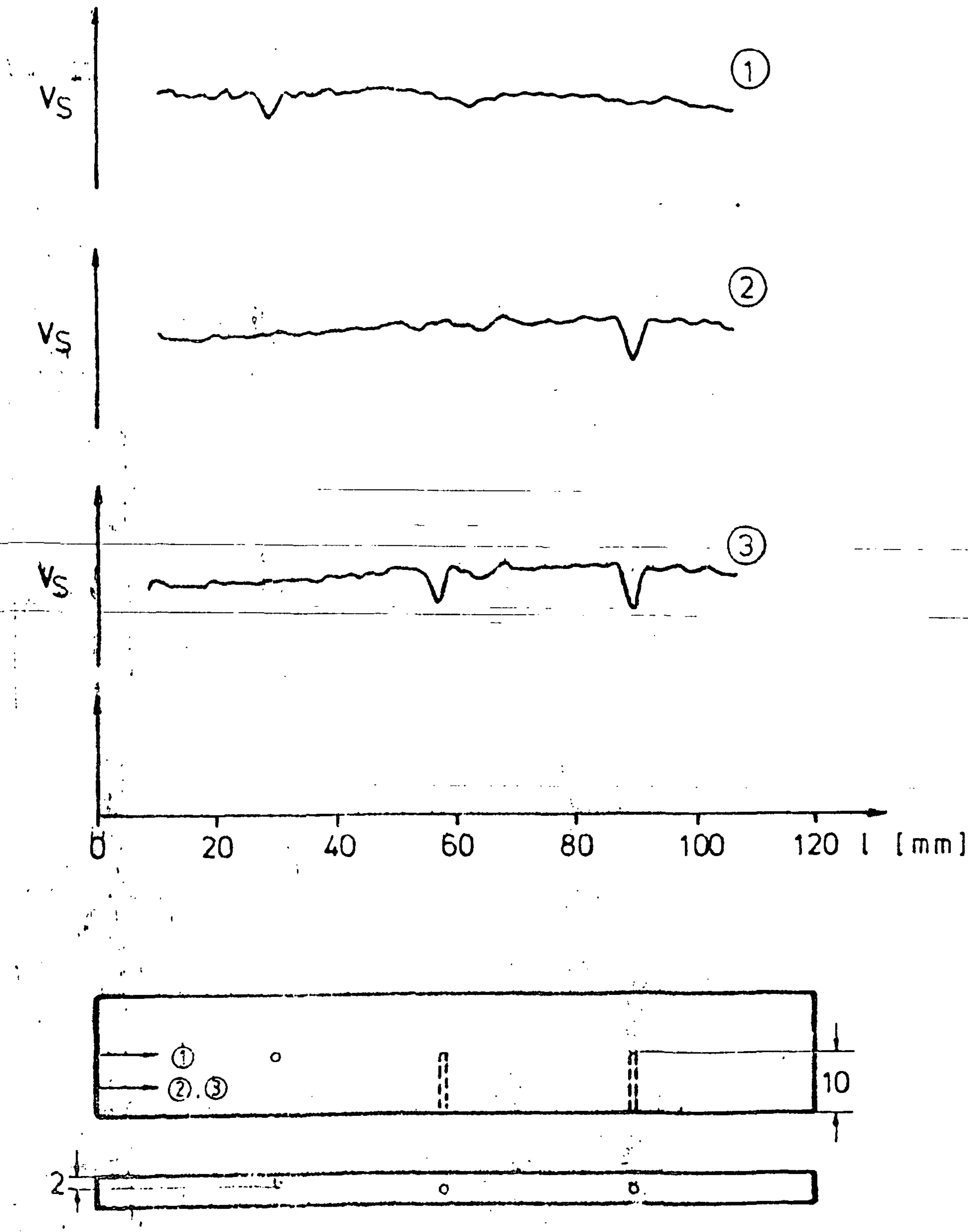

Fig. 23: Microwave tests with an RBSN rod.

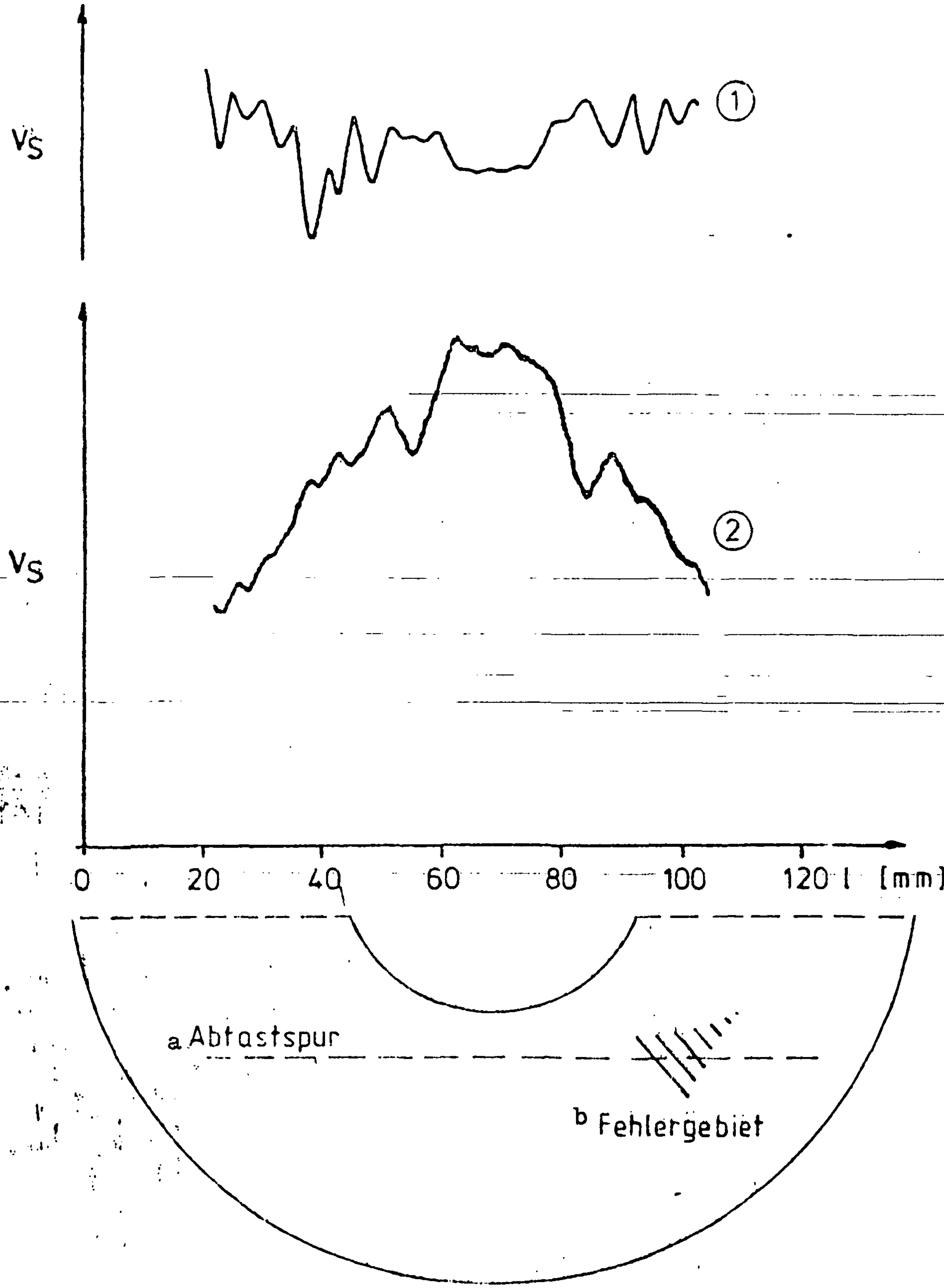

Fig. 24: Microwave test with an RBSN centrifugal disc

Key: a. scanning track
b. defect area

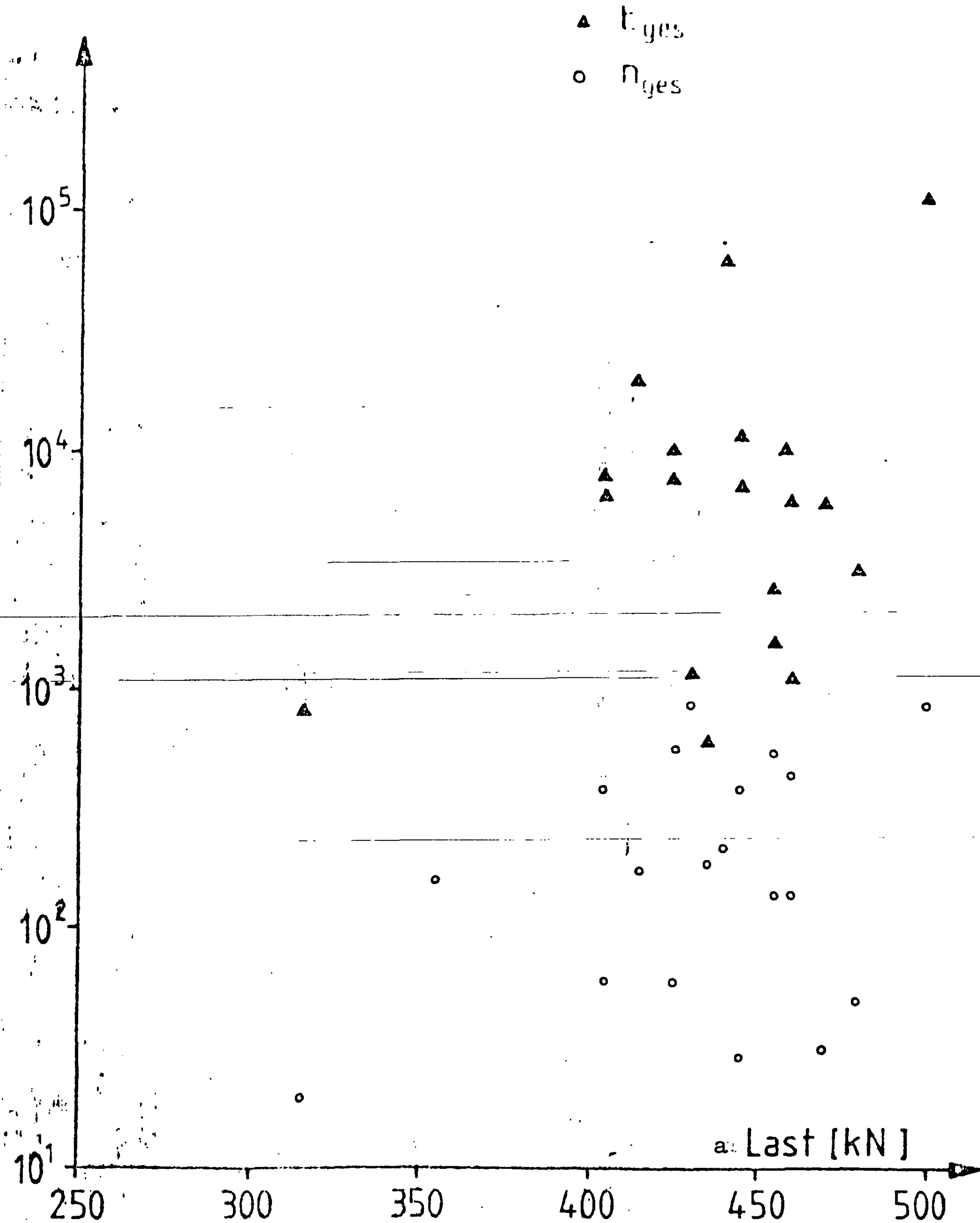

Fig. 25: Energy (E_{ges}) and Event Rate (n_{ges}) as a function of Fracture Load

Key: a. load

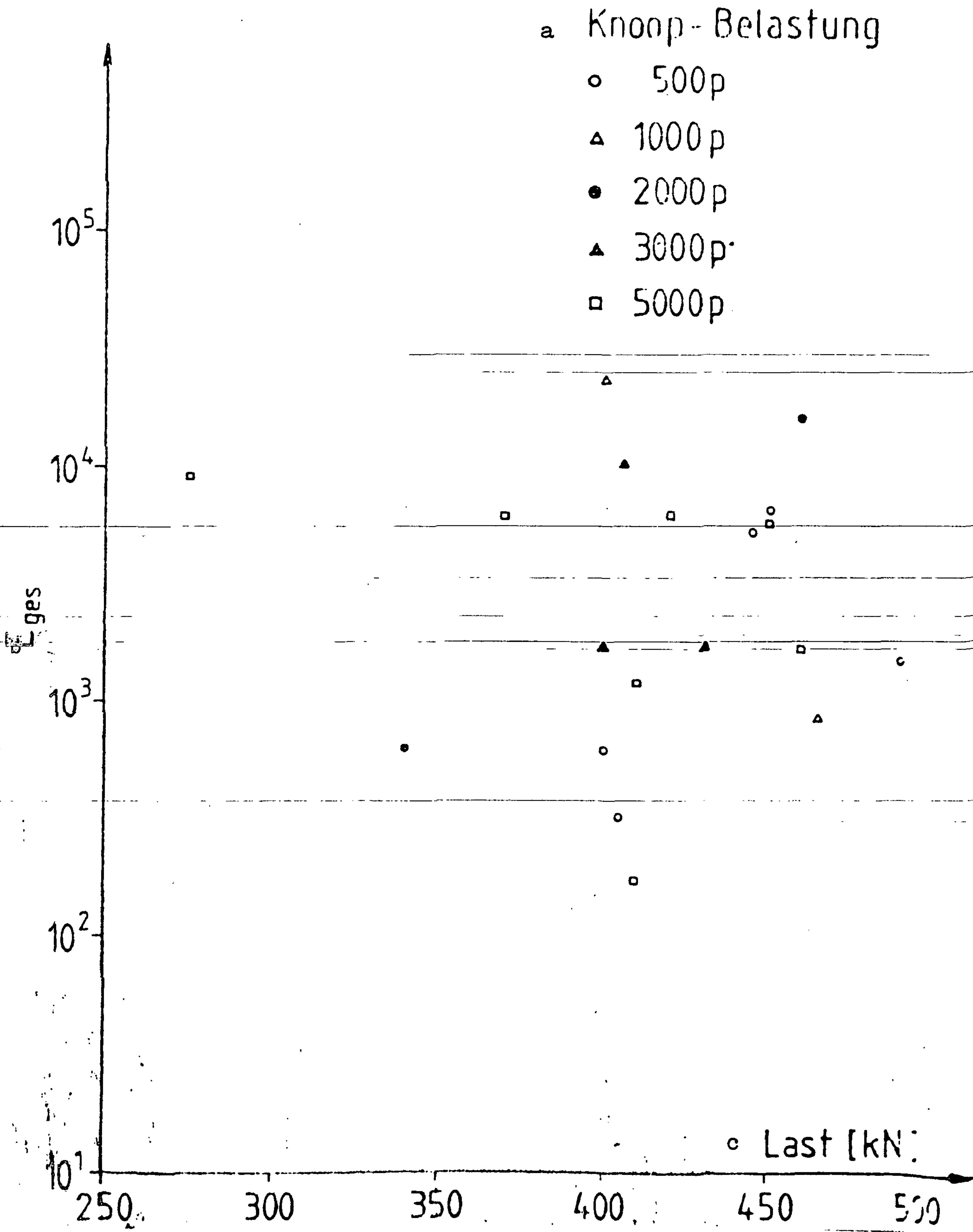

Fig. 26: Energy rate as a function of fracture load with different Knoop loads

Key: a. Knoop load b. total energy c. load

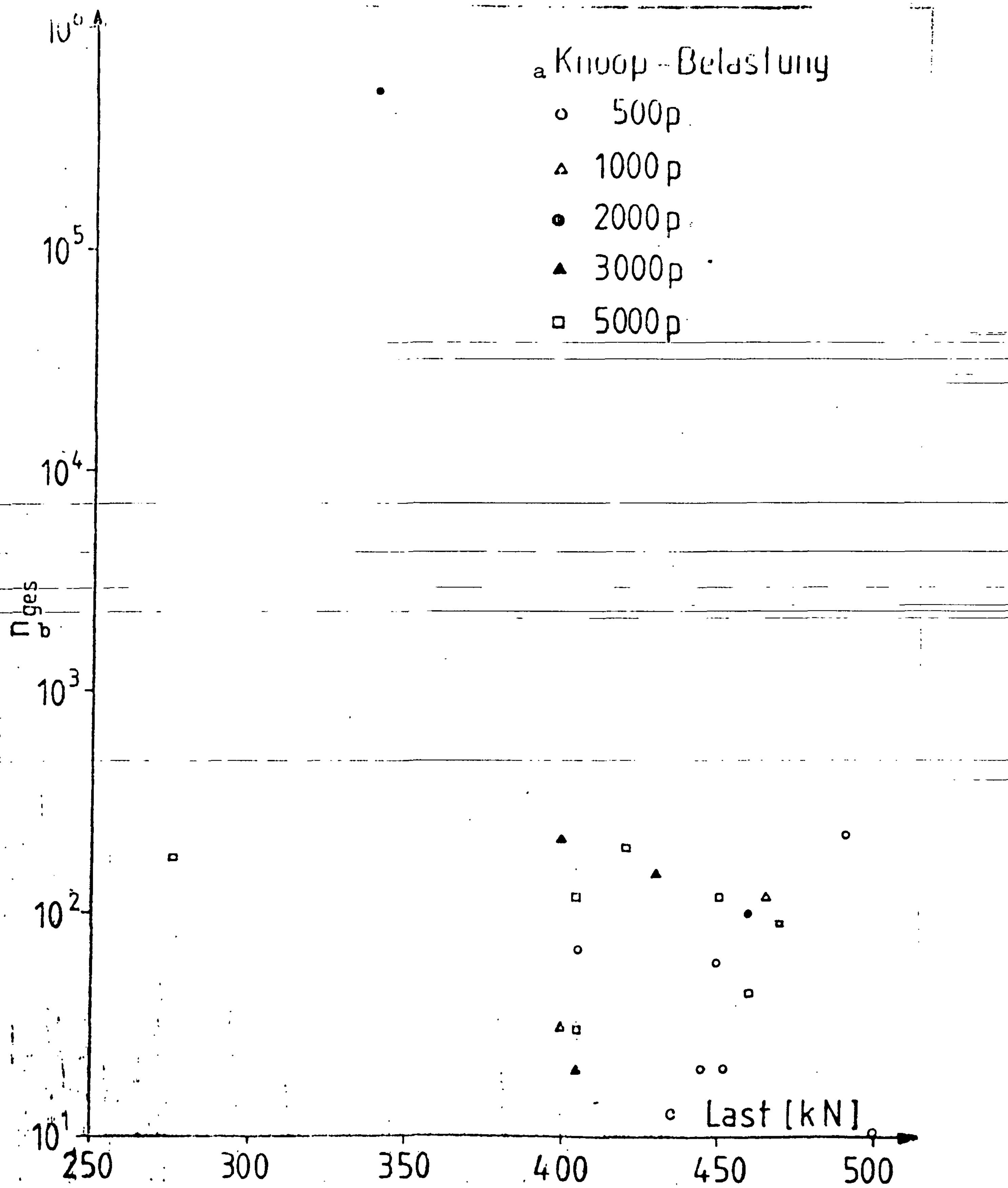

Fig. 27: Rate of Events as a Function of Fracture Load with varying Knoop Loads.

Key: a. Knoop load b. total events c. load

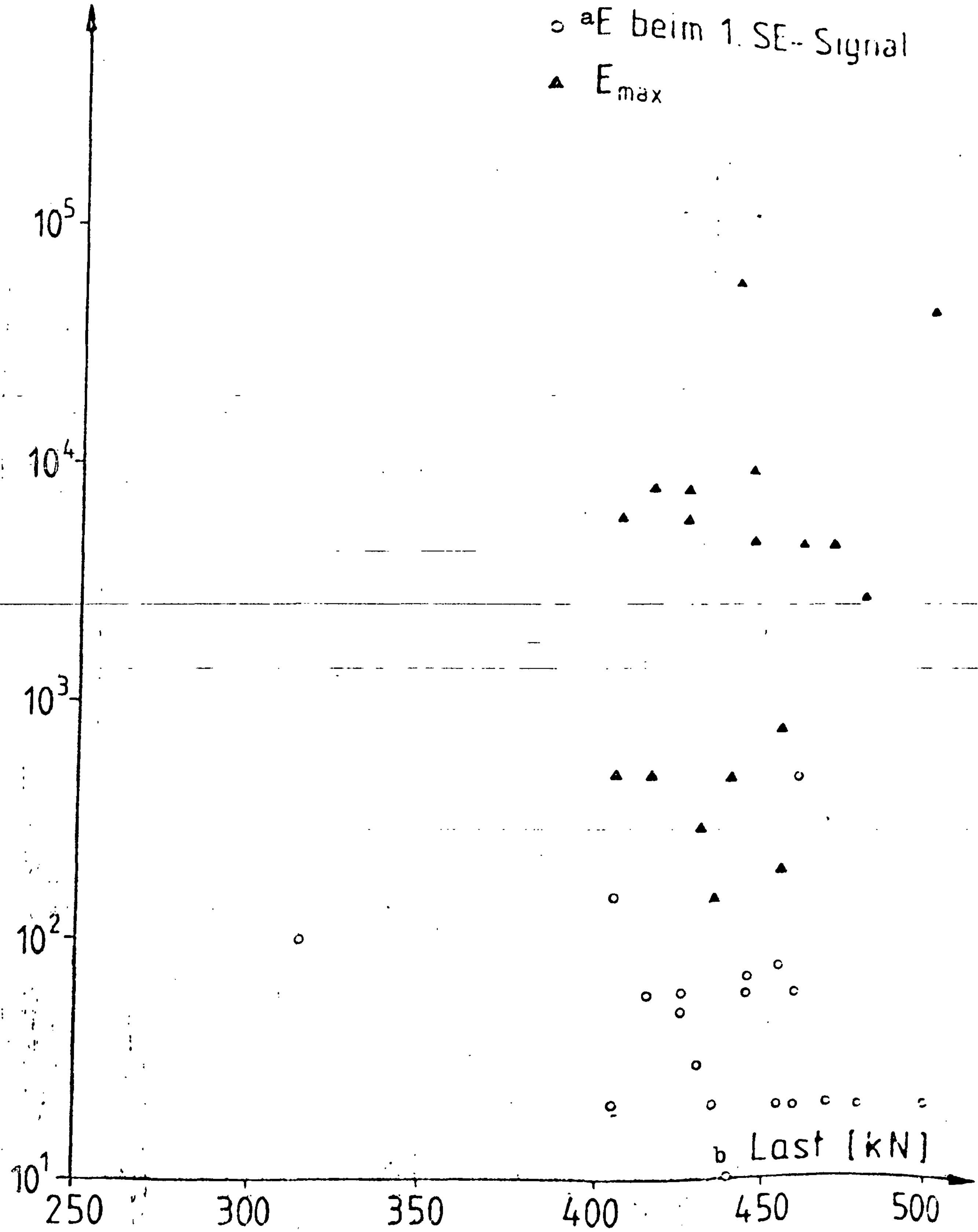

Fig. 28: Energy rate with the first SE signal as well as maximum energy rate as a function of fracture load.

Key: a. energy with the first SE signal
b. load

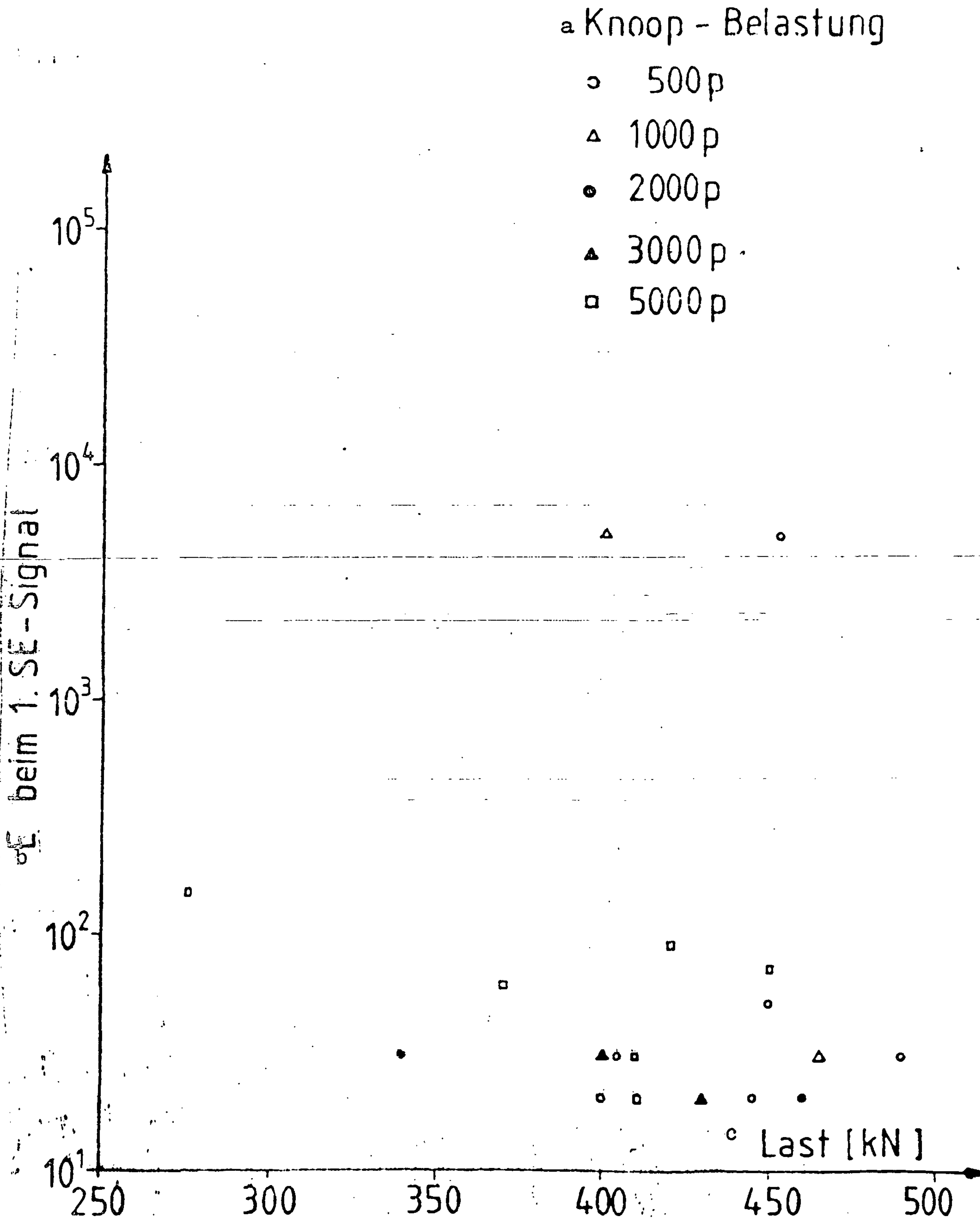

Fig. 29: Energy rate with the first SE signal with varying Knoop load as a function of fracture load.

Key: a. Knoop load b. energy with first SE signal
c. load

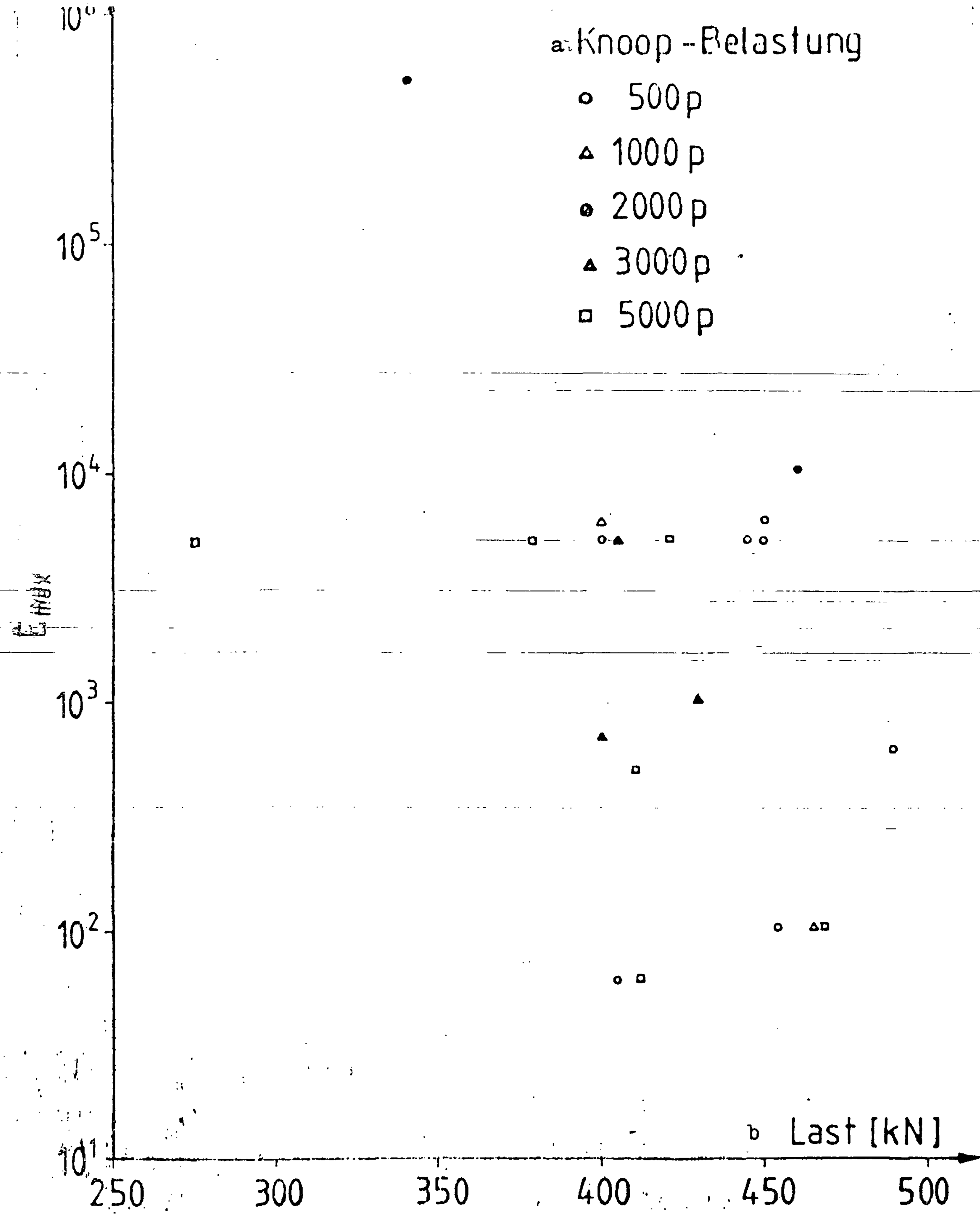

Fig. 30: Maximum energy rate with varying Knoop load as a function of fracture load.

Key: a. Knoop load b. load

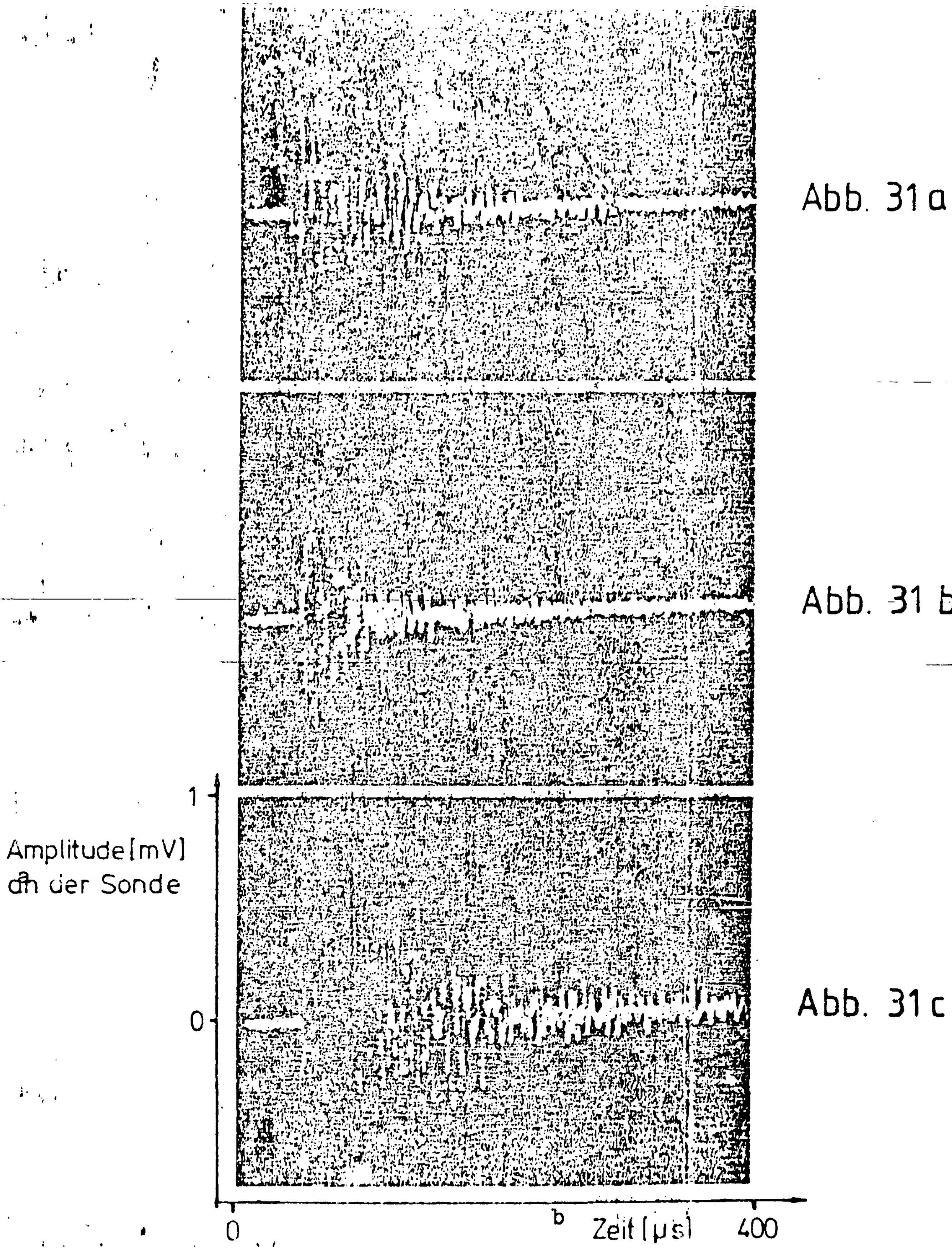

Fig. 31: Sound emission signals, differences in signal form.
Key: a. at the probe b. time

REFERENCES

[1] Reiter, H., K. Goebbels, W. Deuble, "Non-destructive evaluation of high temperature ceramic components for car turbines" IzfP Report No. 790204-TW, Saarbrücken, 1979.

[2] Khuri-Yakub, B.T. and G.S. Kino, "1976 IEEE Ultrasonics Symposium Proceedings," pp. 564-566.

[3] Goebbels, K. and H. Reiter, "Characterization of Defects and Heterogeneities in Si_3N_4 and SiC by Different NDT Methodes", Proceedings of the ARPA/AFML Review of Progress in Quantitative NDE, San Diego, 1979.

[4] Kessler, L.C. and D.E. Yuhas, "Acoustic-Microscopy", 1979 Proc. of the IEEE, 67, 4, pp. 526-536, 1979.

[5] Lemmons, R.A., C.F. Quate, "A Scanning Acoustic Microscope", 1973 IEEE Ultrasonics Symposium Proceedings, pp. 18-21, 1973.

[6] Quate, C.F., "The Ultrasonic Microscope", Spektrum der Wissenschaft 1979, no. 12, pp. 24-33 (1979).

[7] Kupperman, D.S., C. Sciammarella, N.P. Lapinski, A. Sather, D. Yuhas, L. Kessler, N.F. Fiore, "Preliminary Evaluation of Several Nondestructive Evaluation Techniques for Silicon Nitride Gas Turbine Rotors", ANL Report 77-89, January 1978.

[8] Kupperman, D.S., D. Yuhas, C. Sciammarella, N.P. Lapinski, N. Fiore, "Nondestructive Evaluation Techniques for Silicon Carbide Heat-Exchanger Tubes", ANL Report 79-4, March 1979.

[9] Kupperman, D.S., A. Sather, N.P. Lapinski, C. Sciammarella, D. Yuhas, "Preliminary Evaluation of NDE Techniques for Structural Ceramics," Report AFML-TR 78-205, Proceedings ARPA/AFML Meeting, p. 214, 1978.

[10] Truell, R., Ch. Elbaum, B.B. Chick, Ultrasonic Methods in Solid State Physics, Academic Press, New York, 1969.

[11] Hirsekorn, S., "Scattering of even ultrasonic waves at spherical isotropic inclusions in an isotropic medium", IzfP Report No. 780157-TW, Saarbrücken, 1978.

[12] Hirsekorn, S., "Scattering of even ultrasonic waves at spherical isotropic inclusions in an isotropic medium, taking multiple scattering into account", IzfP Report No. 790218-TW, Saarbrücken, 1979.

[13] Tittmann, B.R., Cohen, E.R., Richardson, J.M., J. Acoust. Soc. Am. 63, 68 (1978).

[14] Gubernatis, J.E., E. Domany, J.A. Krumhansl, <u>J. Appl. Phys. 48</u>, 2804 (1977).

[15] Bahr, A.J., "Microwave Techniques for Nondestructive Evaluation of Ceramics", Report AD/A-048 582, AMMRC-CTR-77-29, Nov. 1977.

[16] Lange, E., N. Müller, "Large Scale Production Test of Gas Turbine Components by Injection Molding", Sixth AMMRC Materials Technology Conference Ceramics for High Performance Applications III - Reliability, Orcas Island, Washington, July 1979.